Highly efficient gene expression based on chromatin engineering

クロマチン構造の人為的改変による遺伝子の高効率発現

Studies on Molecular Genetics
Major in Integrative Bioscience and Biomedical Engineering
Graduate School of Science and Engineering
Waseda University

Jun-ichi Tanase
棚瀬　潤一

2010 年 4 月

Contents

Chapter 2

Activation mechanism of chromatin transcription by superhelically curved DNA segments

Abbreviations

Alb	albumin gene
Alox5ap	arachidonate 5-lipoxygenase-activating protein gene
Cdk3	cyclin-dependent kinase 3 gene
ChIP	chromatin immunoprecipitation
CK18	cytokeratin 18
CYC1	iso-1-cytochrome c gene
Cyp7α1	cholesterol 7 alpha hydroxylase gene
DNase I	deoxyribonuclease I
ES	embryonic stem
FGF	fibroblast growth factor
GAPDH	glyceraldehyde-3-phosphate dehydrogenase
GFP	green fluorescent protein
HGF	hepatocyte growth factor
HSV	herpes simplex virus
IPCR	inverse polymerase chain reaction
lacZ	β-galactosidase gene
LIF	leukemia inhibitory factor
MNase	micrococcal nuclease
Neo^{r}	neomycin phosphotransferase gene
Oct4	POU domain, class 5, transcription factor 1 gene
PEPCK	phosphoenolpyruvate carboxykinase 1 gene
Rps18	ribosomal protein S18 gene

RT-PCR	reverse transcription polymerase chain reaction
TAT	tyrosine aminotransferase gene
TBP	TATA binding protein
Tgfbr3	transforming growth factor ß receptor III gene
tk	thymidine kinase gene
UAS	upstream activating sequence
URA3	orotidine-5'-phosphate decarboxylase gene

Abstract

Curved DNA structures with a left-handed superhelical conformation can strongly activate transcription of transgenes in HeLa cells and COS-7 cells. T20 is an artificial 180 bp curved DNA segment of the kind that serves as a transcriptional activator in these cells. In the current study, we firstly investigated the effect of T20 on transcription in mouse embryonic stem (ES) cell lines or hepatocytes differentiated from them. I established ten sets of cell lines each harboring a single copy of the reporter construct. Each set comprised a pair of a T20-harboring cell line and a T20-less control cell line. Analyses showed that in ES cells and in hepatocytes originating from these cells, T20 both activated and repressed transcription in a manner that was dependent on the locus of reporter. The current and previous studies strongly suggest that in cells that have a strict gene regulation system, transcriptional activation by T20 occurs only when the reporter is positioned in a transcriptionally active locus in the genome.

We further studied the effect of curved DNA structures with a yeast mini-chromosome system. Using 108, 180 and 252 bp synthetic curved DNA segments, the mechanism of transcriptional activation by curved DNA structures with a left-handed superhelical conformation has been studied. Even in the presence of nucleosomes, these DNA segments activated transcription from a UAS-deleted *CYC1* promoter that is silenced in the presence of nucleosomes. The fold-activations by these segments, relative to the controls that lacked such segments, were 51.4, 63.4 and 56.4,

respectively. The curved DNA structures with a left-handed superhelical conformation favored nucleosome formation. Interestingly, however, the translational positions of the nucleosomes were dynamic. The high mobility of the nucleosomes on the superhelically curved DNA structures seemed to influence the mobility of the nucleosomes formed on the promoter, and eventually enhanced the access to the center region of one TATA sequence. Functioning as a dock for the histone core and allowing nucleosome sliding seem to be the mechanisms underlying the transcriptional activation in chromatin by curved DNA structures with a left-handed superhelical conformation.

These two studies should provide important clues for designing and constructing artificial chromatin modulators, as a tool for chromatin engineering.

I. Introduction

Multifarious DNA structures are found in the genome. Their implication in DNA packaging and gene expression has long been argued. DNA with a curved trajectory of its helix axis is called bent DNA, or curved DNA. Interestingly, they frequently occur in biologically important regions such as origins of DNA replication, regions that regulate transcription, and recombination loci, and are found in a wide variety of cellular and viral genomes from bacteria to man (1-18). In 1980's and early in 1990's, a vast many studies have been carried out to understand their biological significance and, as the result, their essential roles seem to be largely understood (19-22).

Curved DNA structures are often implicated in transcriptional regulation in both prokaryotes and eukaryotes. In prokaryotes, they are often located from immediately upstream of the -35 hexamer to around position -100 relative to the transcription start site (+1) (23-37). They have a range of functions: facilitating RNA polymerase binding to the promoter, transition from closed to open promoter complexes, or transcription factor binding. To perform these functions, in some cases intrinsically curved DNA structures function together with DNA bends that are induced by binding of RNA polymerase, transcription factors, or nucleoid-associated proteins (23, 38-45).

In eukaryotic transcription, naturally occurring curved DNA structures function in several ways. These include acting as a structural

(conformational) signal for transcription factor binding; juxtaposing the basal transcription machinery with effector domains on upstream-bound factors; regulating transcription in association with transcription-factor-induced bending of DNA; and appropriately organizing the local chromatin structure for transcription initiation (22).

It has been revealed that the shape of the curved DNA is an important factor in transcription. In prokaryotes, right-handed superhelical curvatures activate transcription. These structures help RNA polymerase to bind to promoters and facilitate formation of the open promoter complex (21, 32, 34, 38, 45-51). On the other hand, eukaryotic transcription is sometimes activated by mimicry of negative (left-handed) supercoils; that is, by curved DNA structures with a left-handed superhelical conformation (22, 52-54). Eukaryotic genomes are first folded into nucleosomes, the fundamental unit of chromatin, where DNA forms left-handed supercoils (55, 56). The mimicry of such structures may presumably adjust the local chromatin infrastructure to make it appropriate for transcription initiation and thus can activate transcription (20, 22, 52, 57, 58). Although nucleosomes generally inhibit access or assembly of transcription factors and thus inhibit transcription (59, 60), left-handed superhelical curvatures seem to provide a mechanism to circumvent this problem.

Based on the knowledge described above, curved DNA structures have been thought to provide a basis for “chromatin engineering” for efficient and stable gene expression. The first possibility of chromatin

engineering was found with a synthetic left-handedly curved 36 bp DNA (subsequently named T4) in 2003. This T4 DNA increased the accessibility of the TATA box of the reporter promoter in chromatin, in a transient transfection assay system using COS-7 cells, and activated transcription by about 10-fold (52). Furthermore, when a T4-containing reporter was delivered into mouse liver by a hydrodynamics-based injection, T4 also activated transcription of the reporter gene (53). More interestingly, a recent study found that synthetic left-handedly curved DNA segments of 180 bp (named T20), 216 bp (T24), 252 bp (T28), 288 bp (T32), 324 bp (T36) and 360 bp (T40) are strong activators of transcription (61). These segments activated transcription from the herpes simplex virus (HSV) thymidine kinase (*tk*) promoter by about 70 to 140-fold in a transient transfection assay system in COS-7 cells. The effect of T20 on transcription in the genome chromatin context was also examined by establishment of five HeLa cell lines each harboring a T20-containing reporter in the HeLa genome and five with T20 deleted from the reporter loci. In the T20-harboring cells, transcription of the reporter gene was activated by about 2.5-, 8-, 11-, 21-, and 90-fold, respectively, compared to the control cell lines (61).

With these backgrounds of curved DNA research, the current study aimed to further develop chromatin engineering. Although it was clarified that the curved DNA segments with a left-handed superhelical conformation are definitely effective in some cells, there remain many

issues to be clarified at the very first step of chromatin engineering. Since the results obtained to date show that T20 is a strong activator of transcription, the current study firstly investigated if T20 exerts similar effects in mouse ES cells and whether these effects are maintained after cell differentiation. Secondly, this study investigated the activation mechanism of transcription by T20 using yeast mini-chromosome system (62). Heretofore, the mechanism has not been clarified, except for the case of the short segment T4 (61). This is mainly due to the experimental difficulty in using mammalian cells for fine analyses of chromatin architectures. The principal cause is the size of mammalian genomes. Mammalian genomes are very large and thus require a large amount of DNA to obtain a sufficient molarity for the analyses, which reduces the resolution. Another problem is the lack of convenient episomal systems for analyses of chromatin structure.

The experimental results showed that the chicken *ß-actin* promoter, a well-known strong promoter, could be even activated by T20 in mouse genomic chromatin in both ES cells and the hepatocytes differentiated from them. The activation, however, occurred in a manner that was dependent on the locus of reporter. It was also shown that T20 can markedly activate transcription from a UAS-deleted *CYC1* promoter in yeast chromatin. Functioning as a dock for the histone core and allowing nucleosome sliding seemed to be the mechanisms underlying the transcriptional activation by T20. The current study provides important clues for designing and

constructing artificial chromatin modulators, as a tool for chromatin engineering.

Chapter 1

Competence of T20 as a transcriptional activator in mouse ES cells and hepatocytes differentiated from them

II. Materials and Methods

II-1. Plasmid construction

Plasmid pLHC20/*loxP*/neo/SL constructed from pCX-GFP, pLHC20/*loxP*/cbact/-4 and pLHC20/*loxP*/TLN-6 (61) was used to establish mouse ES integrants.

Construction of pLHC20/*loxP*/cbact/-4

Plasmid pLNX (61) was digested with *Sal*I and *Xho*I to obtain a fragment containing a *loxP* sequence. This fragment was inserted into the *Sal*I site of pCX-GFP. The resulting construct was digested with *Sna*BI and ligated to the *Eco*RI-*Sac*II fragment of pLNX, which also contains a *loxP* sequence. The resulting plasmid was digested with *Afl*III and *Sac*I, and filled with the T20-containing *Kpn*I-*Nru*I fragment of pLHC20/ELN (61) to generate pLHC20/*loxP*/cbact.

Plasmid pLHC20/*loxP*/cbact/-4 is a variant of pLHC20/*loxP*/cbact with a deletion of 4 base pairs between T20 and the downstream *loxP* sequence of pLHC20/*loxP*/cbact. First, a variant fragment was prepared by PCR using pLHC20/*loxP*/cbact and the primers 5'-TAA ACA AAT AGG GGT TCC GC-3' and 5'-ACT CGA GGG CCC ATA TGA CG-3'. The PCR product was digested with *Sal*I and inserted between the *Sal*I and *Sma*I sites of pLHC20/*loxP*/cbact.

Construction of pLHC20/*loxP*/neo/SL

Plasmid pLHC20/*loxP*/TLN-6 (61) was digested with *Hin*cII and the fragment containing the neomycin-resistant gene was inserted into the *Hin*cII site of pUC19 to generate pUC19neo. The *Sal*I and *Hin*dIII fragment of pUC19neo was then inserted between the corresponding sites of pLHC20/*loxP*/cbact/-4 to generate pLHC20/*loxP*/cbact/-4/neo. We adopted the following procedure to delete the extra base pairs between T20 and each *loxP* site in pLHC20/*loxP*/cbact/-4/neo. Initially, the region spanning from the *Eco*T22I site to the downstream *loxP* sequence in the plasmid was amplified by PCR using the primers 5'-ATC TGA GCT CGT CAA TGC ATT TTT CA-3' and 5'-CAT CGC TGC ACA AAA TAA TT-3'. The resulting fragment was digested with *Bgl*II and inserted between the *Eco*RV and *Bgl*II sites in the plasmid, which generated pLHC20/updel. Next, the region spanning from the *Eco*T22I site to the upstream *loxP* site in pLHC20/*loxP*/cbact/-4/neo was amplified by PCR using the primers 5'-GCA GGT TTA AAC AAT GCA TAT AAC-3' and 5'-ATC TCG TCG TGA CCC ATG GC-3'. The resulting fragment was digested with *Cpo*I and *Eco*T22I and ligated between the corresponding sites in pLHC20/updel. The resulting construct was digested with *Eco*T22I, blunted with T4 DNA polymerase and subjected to self-ligation, which generated pLHC20/upcomp. This construct was digested with *Not*I, blunted with S1 nuclease, and digested with *Sal*I. The *Sal*I and *Pma*CI fragment of pLHC20/upcomp (containing T20 and the *loxP* sequence) was inserted between these sites to generate pLHC20/comp. Finally, to construct

multiple cloning sites upstream of the upstream *loxP* site in pLHC20/comp, the synthetic oligonucleotides 5'-TCG ACG CGT CGC GAT CGA TTA ATT AAC TCG AGC TAG CTA CGT A-3' and 5'-TCG ATA CGT AGC TAG CTC GAG TTA ATT AAT CGA TCG CGA CGC G-3' were annealed and inserted into the *Sal*I site of pLHC20/comp to generate pLHC20/*loxP*/neo/SL.

II-2. Generation of mouse ES cell lines

Mouse ES cells were maintained in Glasgow minimum essential medium (G-MEM) supplemented with 10% fetal bovine serum, 0.1 mM 2-mercaptoethanol, 0.1 mM non-essential amino acids, 1 mM sodium pyruvate and 1,000 units/ml of leukemia inhibitory factor (Chemicon, Temecula, CA, USA) on gelatin-coated dish without feeder cells at 37°C in 5% CO_2. They were electroporated with 300 ng of *Sal*I-digested pLHC20/*loxP*/neo/SL at 300 V/150 μF in a cuvette containing 1×10^6 cells in 250 μl of PBS (-) (63-69). Twenty-four hours after electroporation, G418 (Sigma-Aldrich, St. Louis, MO, USA) was added at a final concentration of 200 μg/ml and the culture was continued for 10 days. Colonies of surviving cells were isolated and cultured again for 5 days in the presence of 0.4 mg/ml G418 to establish the cell lines.

Integration of the reporter construct was confirmed by PCR using the primers 5'-GAC AAT CGG CTG CTC TGA TG-3' and 5'-TGC GAT GTT TCG CTT GGT GG-3', which generated a 414-bp fragment when the reporter was present. Colonies harboring a single reporter were selected by Southern blot analysis. We established ten cell lines that were named MES6/T20, MES7/T20, MES25/T20, MES27/T20, MES32/T20, MES40/T20, MES62/T20, MESA2/T20, MESB2/T20 and MESn36/T20. To establish control cell lines, the cells were transfected with pBS185 (Invitrogen, Carlsbad, CA, USA), which expresses Cre recombinase. After cell cloning, T20-deleted clones were selected based on PCR analysis using

the primers described above. The established control cell lines were named MES6, MES7, MES25, MES27, MES32, MES40, MES62, MESA2, MESB2 and MESn36, respectively.

II-3. Determination of transgene loci

Transgene loci were determined using IPCR (Fig.1) (70). Initially, 500 ng of genomic DNA was digested with *Nco*I or *Pst*I. Each digest was purified and self-ligated in a 500 μl reaction mixture containing 500 ng of the digest, 10 units of T4 DNA ligase (TaKaRa, Otsu, Japan), 1 mM ATP and the ligation buffer at 16°C for 15 hr. After ligation, PCR was performed using the primers 5'-ACC GCT TCC TCG TGC TTT A-3' and 5'-CCA ACG CTA TGT CCT GAT AG-3'. Nested PCR was carried out using the primers 5'-TTT ACG GTA TCG CCG CTC CC-3' and 5'-TCC TGA TAG CGG TCC GCC A-3'. The amplified product was purified on a 0.7% agarose gel and sequenced, and the transgene locus was identified. Each locus was confirmed by checking the consistency with sequence data originating from *Nco*I or *Pst*I digestion.

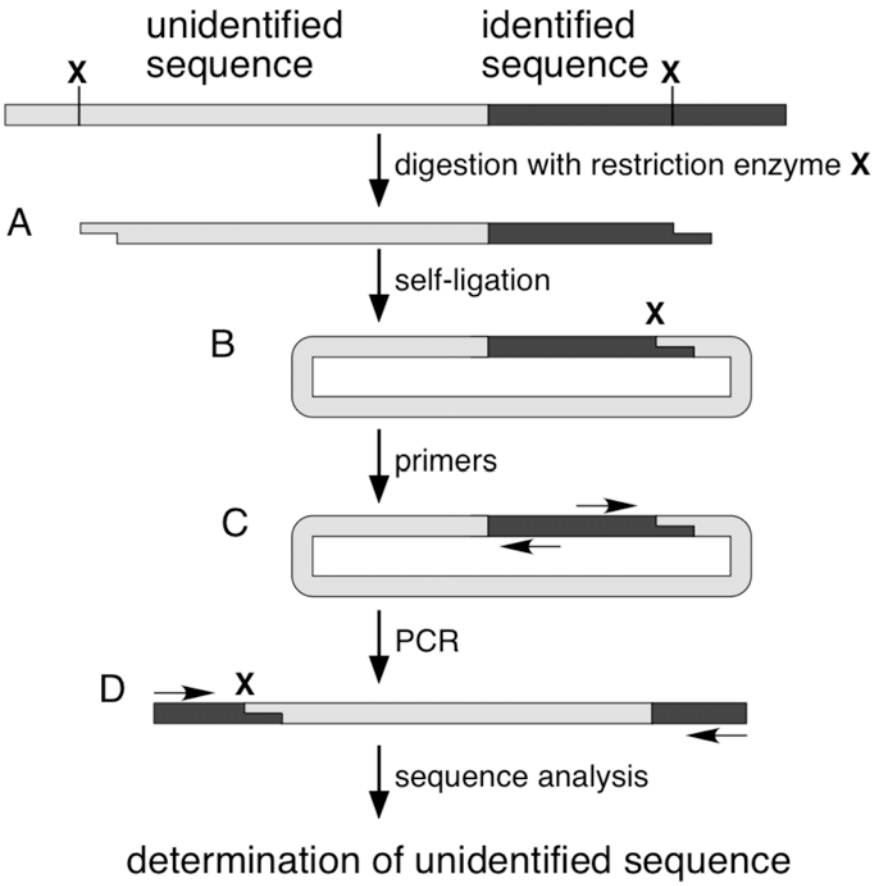

Fig. 1. Inverse RCR

Inverse PCR is an efficient method to determine integration locus of a given transgene. (A) Genomic DNA is digested with restriction enzyme X to contain identified and unidentified sequences. (B) The product is circularized by self-ligation. (C, D) PCR is performed using primers extending outwards. The resulting product is sequenced, which clarifies the integration locus.

II-4. Cell differentiation

The integrants were differentiated into hepatocytes according to the procedure described by Teratani *et al*. (71), with slight modifications. In step 4 of the reported procedure, we cultured cells in Williams medium E containing insulin (5 μg/ml), dexamethasone (100 nM), non-essential amino acids (0.1 mM), L-glutamine (2 mM) and fetal bovine serum (5%) (Fig. 2). Differentiation into hepatocytes was confirmed by detecting expression of hepatocyte-specific genes such as *Alb*, *Cyp7α1*, *PEPCK* and *TAT* using RT-PCR, and *CK18* with immunostaining (72). The RT-PCR was performed as follows. RNA was purified using a conventional method and cDNA was synthesized using 3 μg of total RNA, RevaTra Ace (Toyobo, Osaka, Japan) and oligo(dT). The primers used were as follows: for *Alb*, 5'-CAG GAT TGC AGA CAG ATA GTC-3' and 5'-GCT ACG GCA CAG TGC TTG-3'; for *Cyp7α1*, 5'-CCA CCT TTG ATG ACA TGG AGA AG-3' and 5'-TTC TTC AGA GGC TGC TTT CAT TG-3'; for *PEPCK*, 5'-CAA GTG CCT GCA CTC TGT GG-3' and 5'-CCA CCA TAT CCG CTT CCA AA-3'; for *TAT*, 5'-ACC TTC AAT CCC ATC CGA-3' and 5'-TCC CGA CTG GAT AGG TAG-3'. For immunostaining, cultured cells were fixed in 4% paraformaldehyde at room temperature (RT) for 10 min and then washed three times with 0.1% Triton/PBS (-) at RT for 10 min. Subsequently, the cells were soaked in 5% skimmed milk/PBS (-) at RT for 1 hr, and then washed as above. Cells were incubated with goat anti-mouse CK18 (1:100) (Santa Cruz Biotechnology,

Santa Cruz, CA, USA) at 4°C for 12 hr. After washing, the cells were treated with 0.1% BSA/PBS (-) containing donkey anti-goat IgG-FITC (1:250) (Santa Cruz Biotechnology) at RT for 1 hr, washed as described above, and sealed with Vectashield Mounting Medium with DAPI (Vector, Burlingame, CA, USA).

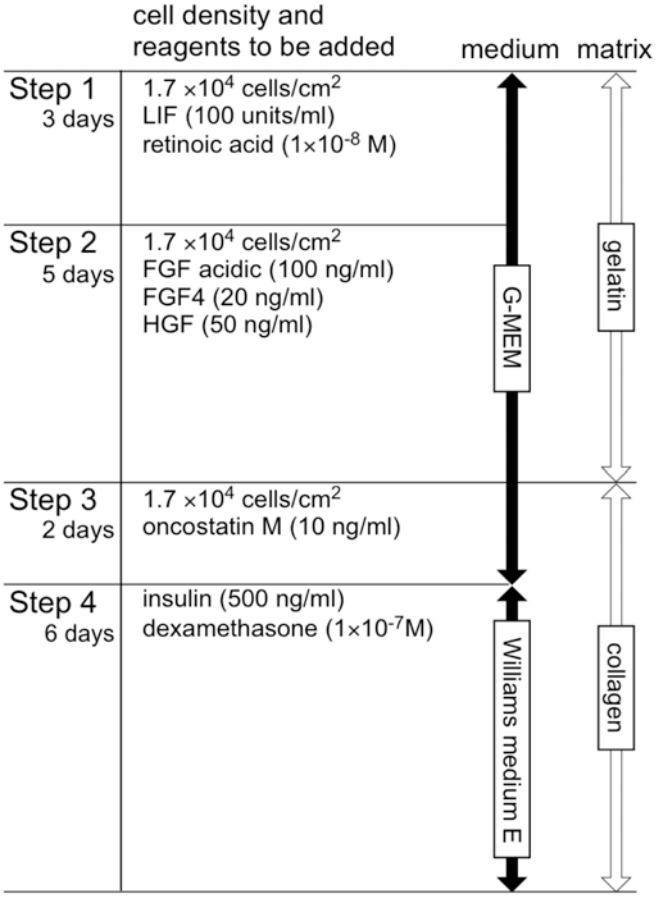

Fig. 2. The method for inducing differentiation of mouse ES cells into hepatocytes
Cell differentiation was completed in 16 days. About 60-70% mouse ES cells differentiated into hepatocytes by this method.

II-5. Quantitative real-time PCR analysis

GFP mRNA was purified from ES cells or hepatocytes and cDNA was synthesized as described above. The product was quantified by SYBR Green with normalization against the housekeeping gene *Rps18*, using a StepOne Plus real-time PCR system and StepOne software v. 2.1 (Applied Biosystems, Carlsbad, CA, USA). The following primers were used: for GFP mRNA, 5'-TTG GCG ATG GCC CTG TC-3' and 5'-ACC TGA GGA GTG AAT TC-3'; for *Rps18* mRNA, 5'-CCT GAG AAG TTC CAG CAC AT-3' and 5'-TTC TCC AGC CCT CTT GGT G-3'.

II-6. DNase I footprinting assay

Nuclei were prepared as described previously (5, 52). Aliquots of 100 μl nuclear suspension (1×10^7 nuclei/ml) were incubated at 37°C for 1 min. Then, 0.05 U, 0.1 U or 0.3 U of DNase I was added and digestion was performed at 37°C for 2 min. Naked DNA was digested with 0.001 U, 0.003 U or 0.005 U of DNase I. After digestion, the products were purified and dissolved in water at 1 mg/ml. To detect DNase I cleavage sites, ligation-mediated PCR (73) was carried out using 3 μg DNase I digests as follows. A primer DNA of sequence 5'-TCA CCT GTG GGA GTA ACG CG-3' was hybridized to the digests and extended to the cleavage sites with KOD-plus (Toyobo, Osaka, Japan) at 68°C for 10 min. Then, a 25-bp linker DNA was ligated to the resulting products and PCR was carried out using the primers 5'-GCG GTG ACC CGG GAG ATC TGA ATT C-3' and 5'-AAC GCG GTC AGT CAG AGC CG-3' under the following conditions: 98°C for 2 min and 30 cycles at 98°C for 30 sec, 58°C for 30 sec and 68°C for 2 min. Subsequently, DNase I cleavage sites were detected by PCR-based primer extension using a [5'-^{32}P]-labeled primer, 5'-TCA GTC AGA GCC GGG GCG GG-3', under the following conditions: 98°C for 2 min and 20 cycles at 98°C for 30 sec, 63°C for 5 sec and 74°C for 30 sec. All samples were purified and resolved in 6% polyacrylamide-7 M urea gels.

II-7. ChIP assay

The ChIP assay was performed according to Chadee *et al*. (74) with slight modifications. Nuclei were prepared as reported by Nishikawa *et al*. (52) and aliquots of 50 µl nuclear suspension (4 $\times 10^7$ nuclei/ml) were digested with 10 U of MNase at 37°C for 15 min. Then, 50 µl of 2× lysis buffer comprising 150 mM NaCl, 25 mM Tris-HCl (pH 7.5), 5 mM EDTA, 1% Triton X-100, 0.1% SDS, and 0.5% sodium deoxycholate was added to the reaction mixture and incubated at 4°C for 10 min. Immunoprecipitation was carried out in triplicate using a OneDay ChIP Kit (Diagenode, Liège, Belgium) according to the manufacturer's instructions, using antibody against histone H3 (ab1791; Abcam, Cambridge, UK). Using 2 µl of the DNA samples thus obtained, quantification of fragments containing a part of the chicken *ß-actin* promoter (R1, R2 and R3) was carried out by SYBR green quantitative real-time PCR with the StepOne Plus real-time PCR system and StepOne software v. 2.1. Quantification of fragments containing a part of *GAPDH* was carried out simultaneously as an internal control. The primer sets were as follows: for R1, 5'-TCT CCG TAT TAG TCA TCG C-3' and 5'-CAT CGC TGC ACA AAA TAA TT-3'; for R2, 5'-AAT TAT TTT GTG CAG CGA TGG-3' and 5'-CGC CTC GCC ATA AAA GGA AAC T-3'; for R3, 5'-GCG CTC CGA AAG TTT CCT TTT A-3' and 5'-TCA CCT GTG GGA GTA ACG CG-3'; for *GAPDH*, 5'-CCG CAT CTT CTT GTG CAG T-3' and 5'-TCC CTA GAC CCG

TAC AGT GC-3'. The relative sample enrichment was calculated using the formula: $2^{-(\text{Ct target region-Ct GAPDH})}$.

III. Results

III-1. Effect of T20 on transcription in the genome chromatin context

The reporter construct is shown in Fig. 3. The T20 sequence was placed between two *loxP* sequences (75-82) and the resulting sequence was placed upstream of the chicken *ß-actin* (82) promoter linked to the GFP gene. The *loxP* sequences were used to establish control cell lines with a reporter gene without T20. After the construct was cleaved at the *Sal*I site, it was introduced into mouse ES cells. We screened for cell lines with a single copy of the reporter construct using Southern blot analysis (Fig. 4). The following ten cell lines were established: MES27/T20, MES6/T20, MES62/T20, MES32/T20, MES25/T20, MESB2/T20, MES7/T20, MESA2/T20, MESn36/T20 and MES40/T20. The reporter was found integrated immediately upstream of a gene (MES32/T20, MES25/T20, MES7/T20; referred to as group A) or within a structural gene (MES62/T20, MES40/T20; group B) or in an intergenic region (MES27/T20, MES6/T20, MESB2/T20, MESA2/T20, MESn36/T20; group C) (Fig. 5). Control cell lines were established by expressing bacteriophage P1 Cre recombinase in the T20 cell lines. These were named MES27, MES6, MES62, MES32, MES25, MESB2, MES7, MESA2, MESn36 and MES40, respectively (Fig. 6). Differentiation of each cell line into hepatocytes was confirmed by the expression of genes such as *Alb, Cyp7α1, PEPCK, TAT* and *CK18* (Fig. 7, 8) (71).

Expression of the reporter gene (GFP) was analyzed by RT-PCR in undifferentiated and differentiated cells, and GFP mRNA levels were compared between T20-harboring and T20-less cells. As shown in Fig. 8A, in which the data are aligned in the order of activation, four T20-harboring ES cell lines showed higher transcription (MES32/T20, MES25/T20, MESA2/T20, MES7/T20) and three showed lower transcription (MES27/T20, MES40/T20, MES6/T20) compared with respective control cell lines. The fold activations of transcription relative to controls in the four cell lines with higher transcription were 2.7, 1.9, 1.7 and 1.5, respectively, and three of these cells lines were in group A. Since the chicken *ß-actin* promoter is a strong promoter (83-85), these activations are not necessarily small (discussed below). In MES32/T20, MES25/T20 and MES7/T20, the reporter construct was integrated immediately upstream of a gene: upstream of *Tgfbr3* in MES32/T20; *Alox5ap* in MES25/T20; and *Cdk3* in MES7/T20 (Fig. 5). These genes are expressed in ES cells or blastocysts (86-88). The transcription level relative to the control was unchanged in MESn36/T20 and MESB2/T20. Transcription of the reporter gene was not detected in MES62/T20 and MES62; thus, these data are not shown in Fig. 8A. The RIKEN cDNA 4930564D02 gene may not be expressed in ES cells. Except for MESA2/T20, transcriptional stimulation was not observed when the T20-harboring reporter was integrated into an intergenic region or within a structural gene.

Upon cell differentiation into hepatocytes, the effect of T20 greatly changed on the whole (Fig. 8B). For comparison, the data are shown in the same order as those in Fig. 8A. Among the differentiated MES32/T20, MES25/T20, MESA2/T20 and MES7/T20, which showed higher GFP mRNA levels than their controls before differentiation, only MES32/T20 maintained the similar fold of activation of GFP transcription relative to the control. The value slightly fell for MES7/T20 and it was 0.59 for MESA2/T20, which was the strongest transcriptional repression caused by T20. Using RT-PCR, we also clarified that the *Alox5ap* and *Cdk3* were expressed in the hepatocytes differentiated from the ES cells (Fig. 9). The *Tgfbr3* expression in hepatocytes was previously reported (89).

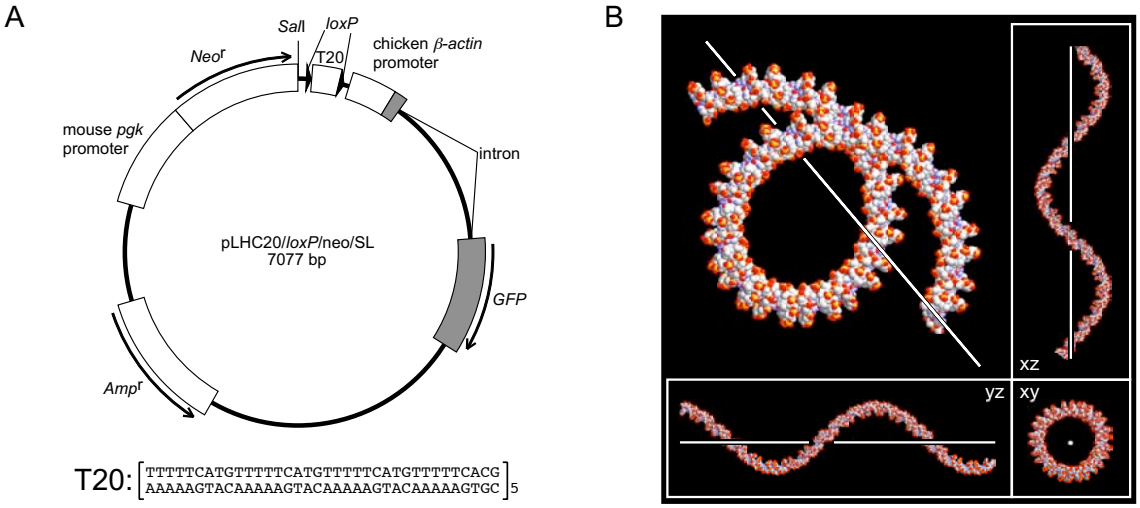

Fig. 3. Reporter construct and architecture of T20

(A) Reporter construct. GFP, *Neo*^{r}, *pgk*, and *loxP* indicate genes encoding green fluorescent protein, neomycin phosphotransferase, phosphoglycerate kinase, and *loxP* sequence, respectively. Nucleotide sequence of T20 is slightly different from that in the previous report (61): the sequence started with 5'-TCAGTTTTT and ended with TTTTT-3' in the previous T20, but the corresponding sequences are TTTTT and TTTTTCACG-3' in the present T20. Since they have the same three-dimensional architecture, the same name was used for convenience. (B) Three-dimensional architecture of T20. The figure was drawn as reported by Sumida *et al*. (61). The white line indicates the superhelical axis.

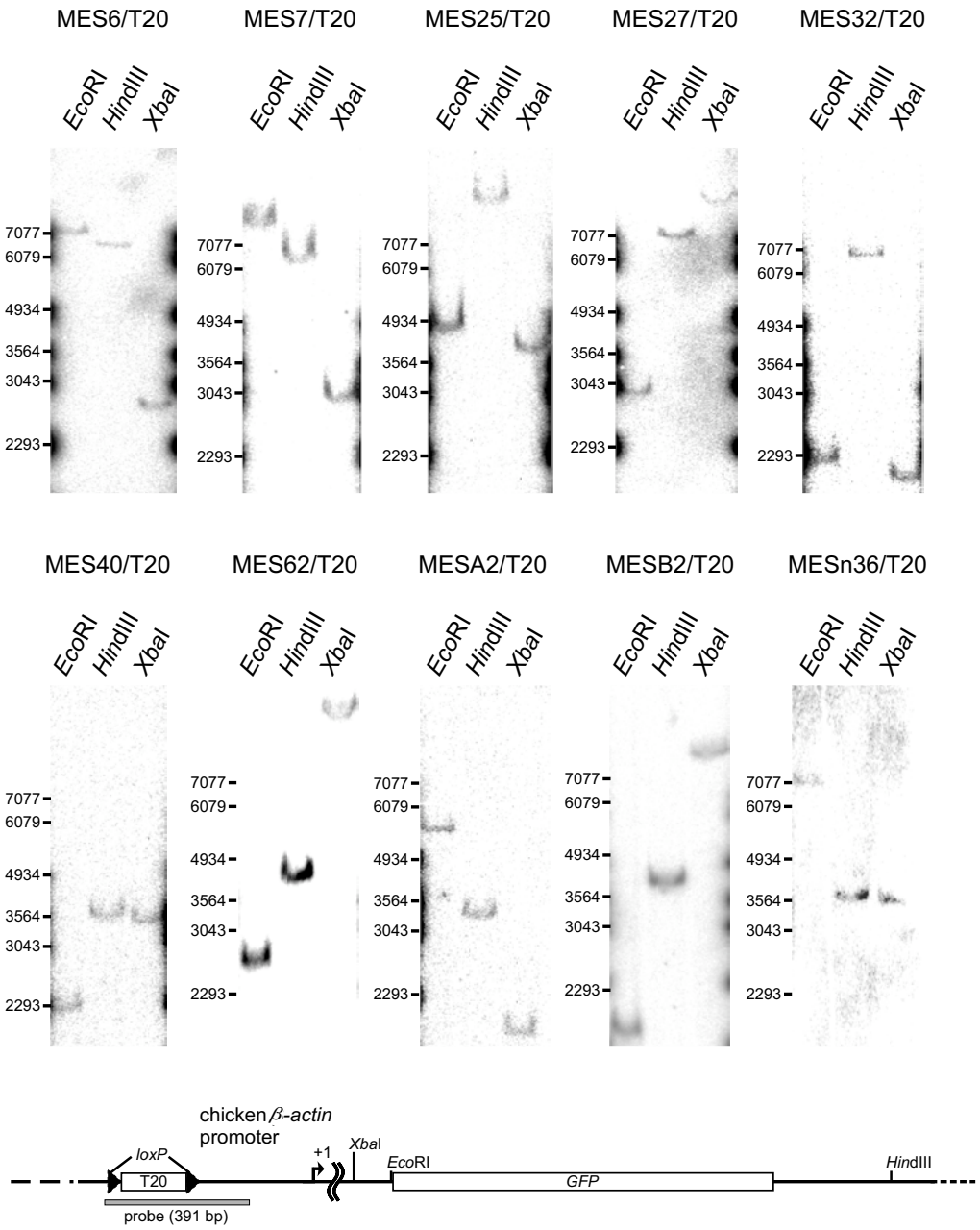

Fig. 4. Southern blot analysis of the reporter construct

Genomic DNAs from the established cell lines were digested with restriction enzymes indicated in the figure. After separation by agarose gel electrophoresis and blotting, each digest was hybridized with a probe indicated below the autoradiograms.

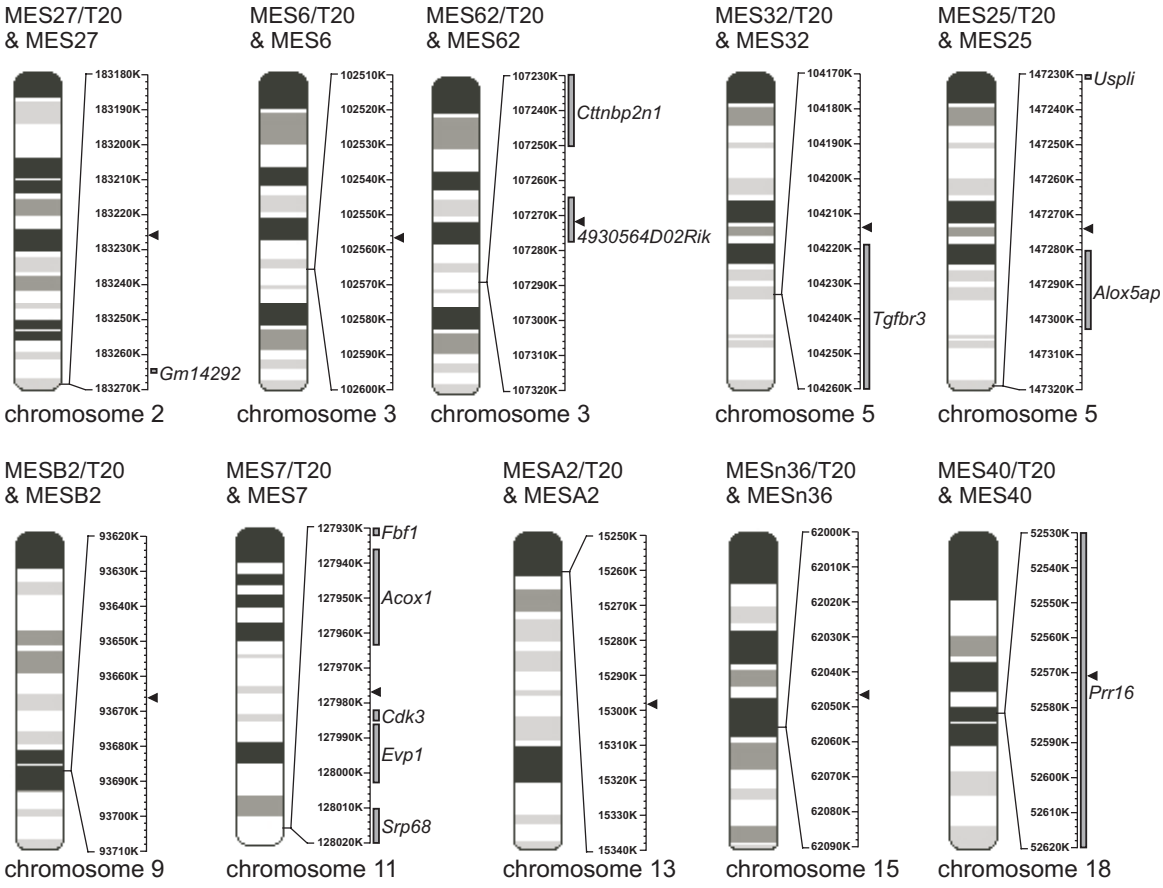

Fig. 5. Locus of the reporter construct in each cell line

The genomic region harboring the reporter construct was identified as described in the Materials and Methods. Loci of integration are indicated with arrowheads.

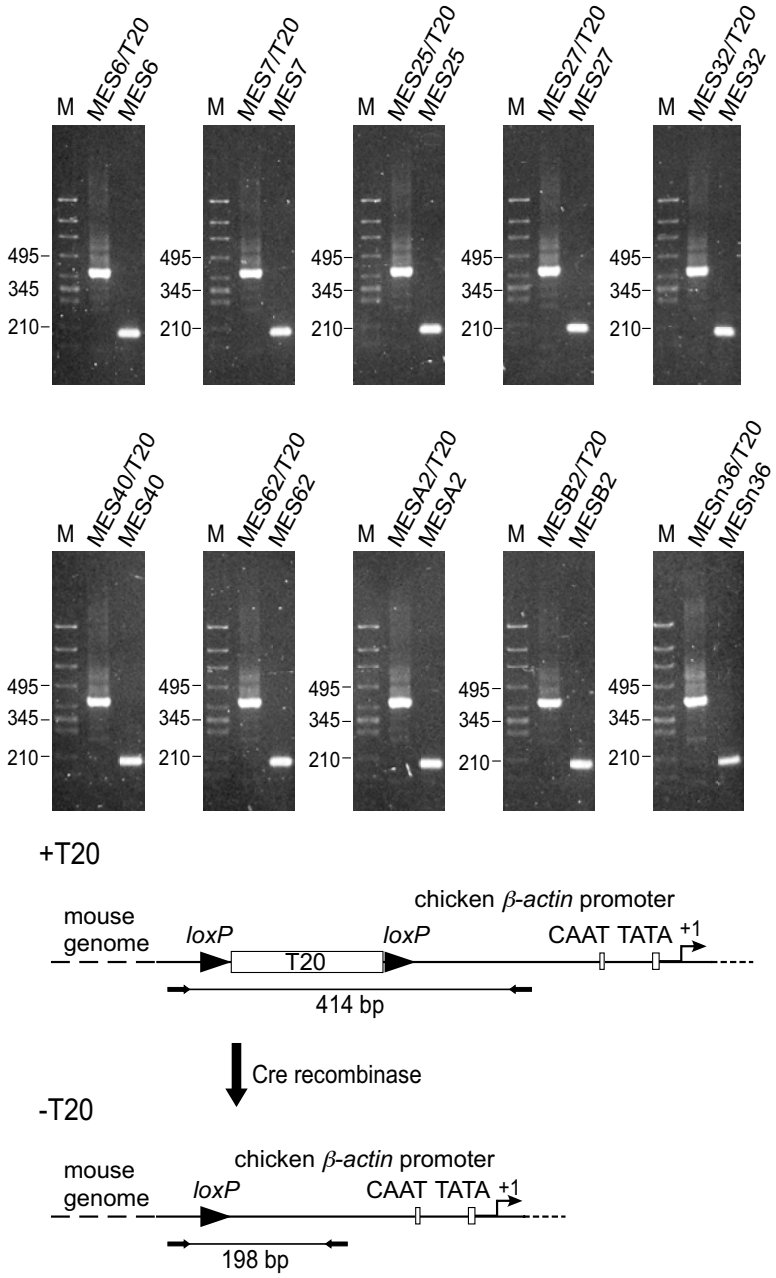

Fig. 6. Establishment of T20-less cell lines

Deletion of T20 from the reporter locus was confirmed by PCR. "M" indicates the size marker lane. The amplified region is shown on the right.

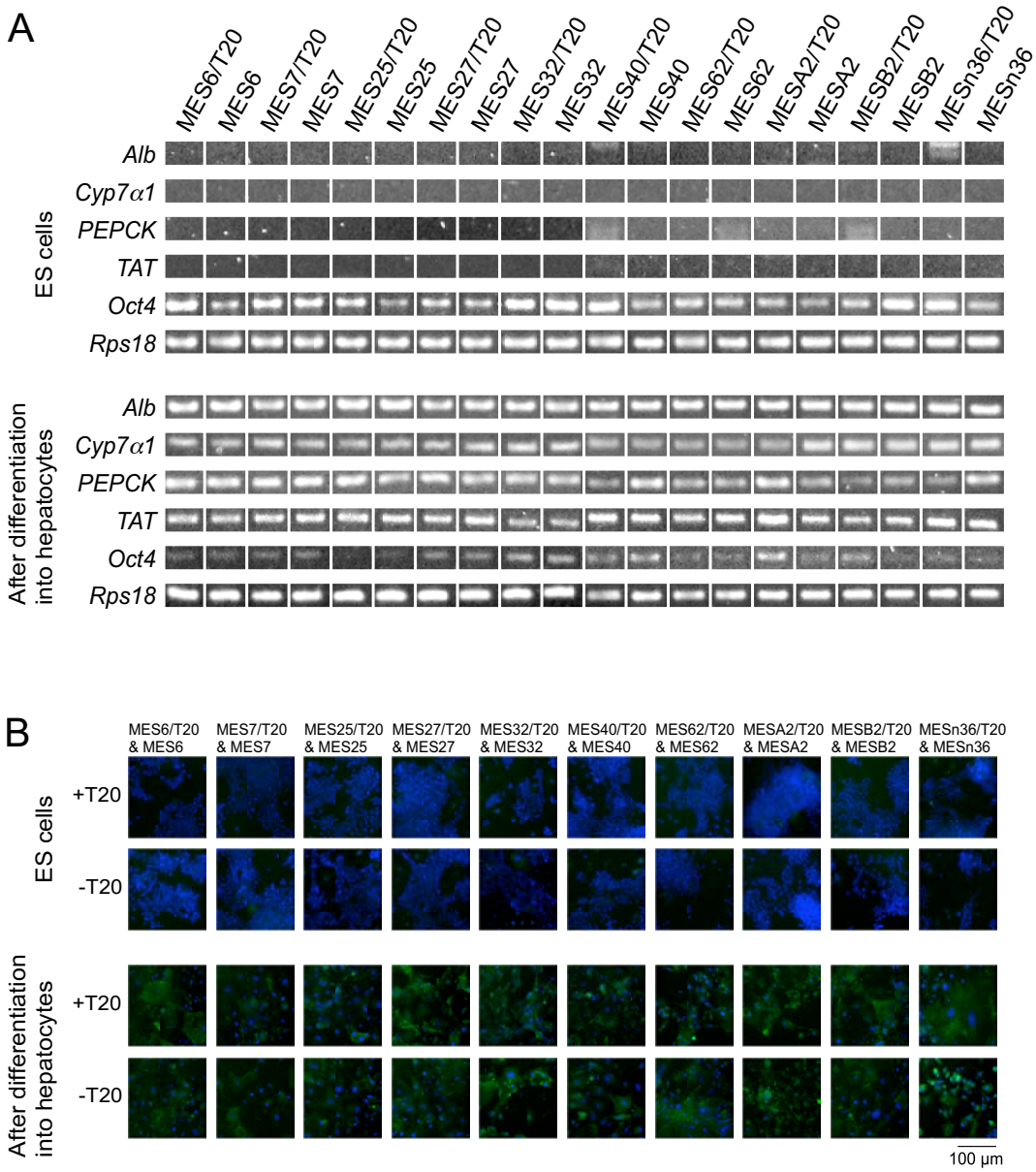

Fig. 7. Differentiation of mouse ES cells into hepatocytes

(A) RT-PCR analyses of mRNA expression of hepatocyte-specific genes *Alb, Cyp7α1, PEPCK,* and *TAT*. *Oct4* is an undifferentiated cell marker and *Rps18* is a housekeeping gene encoding the ribosomal protein S18. The latter was used as an internal control. (B) Immunofluorescent detection of expression of CK18, a marker for hepatocytes, using anti-mouse CK18 antibody (green). Nuclei were stained with DAPI (blue).

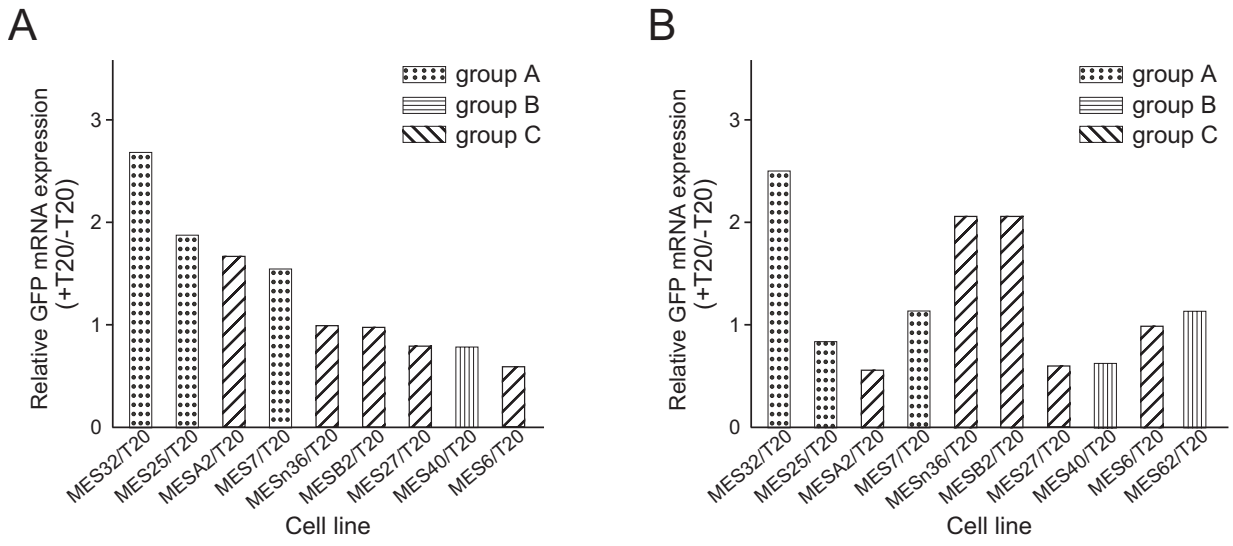

Fig. 8. Effect of T20 on the transcription of reporter gene before or after cell differentiation.

(A) Effect of T20 on transcription of reporter gene in mouse ES cells. At first, expression level of reporter mRNA in each cell line was determined using that of *Rps18* mRNA for normalization. The determinations were carried out in quintuplicate and the mean values ± SD were calculated. Then, the relative GFP mRNA expression (+T20/-T20) was calculated by dividing the expression level of reporter mRNA in each T20-harboring cell line by that in the corresponding control (T20-less) cell line (only mean values were used in the calculation). The dotted, lined and striped bars indicate groups A, B and C, respectively. These groups were established based on the integration locus (see text). (B) Effect of T20 on transcription of reporter gene in hepatocytes differentiated from respective integrants.

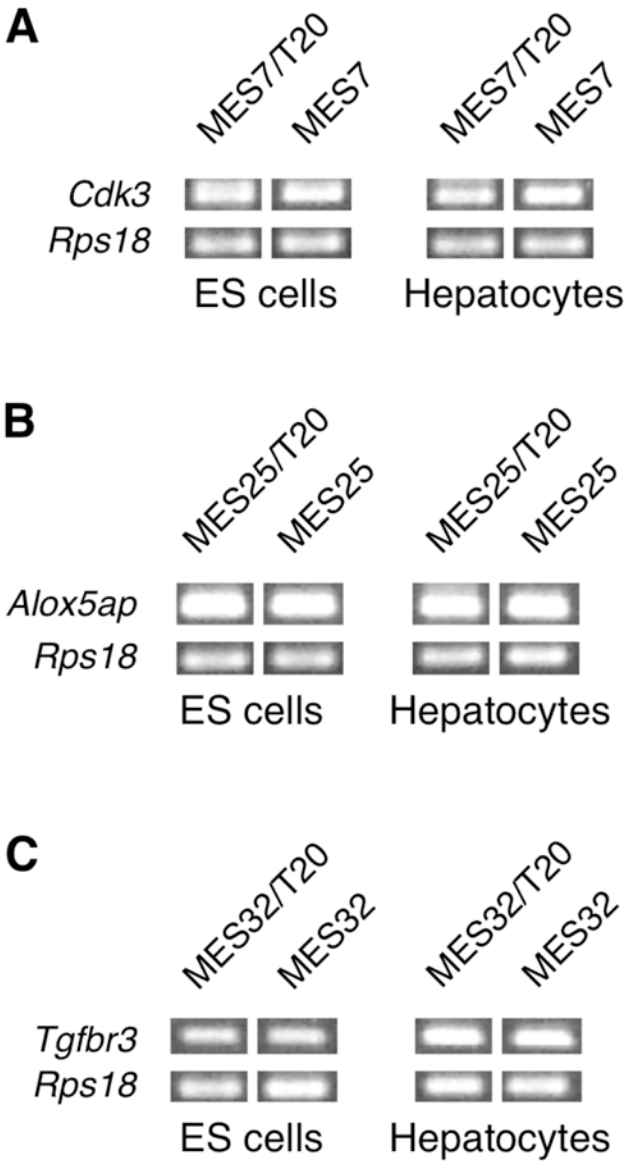

Fig. 9. Expression of the gene adjacent to a transgene

RT-PCR was used for the analysis using undifferentiated and differentiated states of cells. All genes were found to be expressed in both states. (A) *Cdk3* expression in the cell lines MES7/T20 and MES7; (B) *Alox5ap* expression in the cell lines MES25/T20 and MES25; (C) *Tgfbr3* expression in the cell lines MES32/T20 and MES32.

III-2. Chromatin structure on the reporter promoter

The local chromatin structure on the reporter promoter was analyzed by ChIP assay in MES32/T20 and MESA2/T20 cells and their controls. The assay targeted histone H3. MES32/T20 was chosen because the reporter gene was located close to an active gene and transcription of the reporter gene was most activated by T20. MESA2/T20 was chosen because the reporter gene was integrated into an intergenic region and because T20 acted both positively (before differentiation) and negatively (after differentiation) (Fig. 8). The results of the assay are shown in Fig. 10, where the histone level is represented as fold enrichment relative to the level in a region within the GAPDH gene.

For the MESA2/T20 and MESA2 pair (Fig. 10C, D), each region of MESA2/T20 contained less histones in ES cells (Fig. 10C) and more histones in hepatocytes (Fig. 10D) compared to MESA2, which correlated well with the difference in reporter gene expression (Fig. 8). In contrast, for the MES32/T20 and MES32 pair (Fig. 10A, B), only a slight difference in histone levels was observed between the two cell lines in ES cells and hepatocytes; however, the reporter transcription level differed considerably (Fig. 8). Thus, the histone profiles for MESA2/T20 and MESA2 agreed well with the established view that a high histone level has a negative effect on transcription. However, those for MES32/T20 and MES32 could not explain the transcriptional difference between them. To understand the mechanism underlying the greater expression of the reporter gene in

MES32/T20 than in MES32, we then performed DNase I footprinting using isolated nuclei. This assay provides information on the DNA exposed to or shielded from the environment in the complex with proteins including histones. In this experiment, cleavage sites were detected by a combination of ligation-mediated PCR and primer extension (73).

No 10-bp ladder was detected in the footprinting assay (Fig. 11), indicating at least that rotationally positioned nucleosomes were not present in the region analyzed (52). In this assay, the direction of primer extension was towards the region upstream of the reporter gene. MES32/T20 and MES32 had very similar band patterns under the same state of differentiation. Before differentiation of these cells, the extended bands were generally short and remained about 15 to 30 bp upstream of the TATA box (lane 5 in each gel). Furthermore, the extent of digestion of these samples was similar to those of naked DNA samples. Thus, it was suggested that the local chromatin formed on the promoter in each cell line was relatively free from stably bound proteins before differentiation. However, considering that the bands were clearer for MES32/T20 than for MES32, MES32/T20 may have a more ordered complex with some proteins in the TATA box region compared to MES32 in the undifferentiated state, which may explain the higher transcription in the former. After differentiation of MES32/T20 and MES32, the extended fragments reached far upstream from the TATA box, near to the end of the gel (around position -110; lane 8 in each gel) and generated many discrete

bands, indicating that the major population of promoter chromatin formed an ordered structure in the hepatocytes. After differentiation, the reporter gene transcription increased dramatically in these two cell lines (Fig. 12). Thus, the ordered chromatin structure seems to have been indeed implicated in the transcriptional activation. The extended fragments in lane 8 in each gel were slightly longer and clearer for MES32/T20 than for MES32. This difference may also explain the higher transcription in the former. The emerging bands were similar in the region downstream from the transcription start site (+1) in ES cells and hepatocytes, indicating at least that downstream chromatin was not influenced by differentiation in both cell lines.

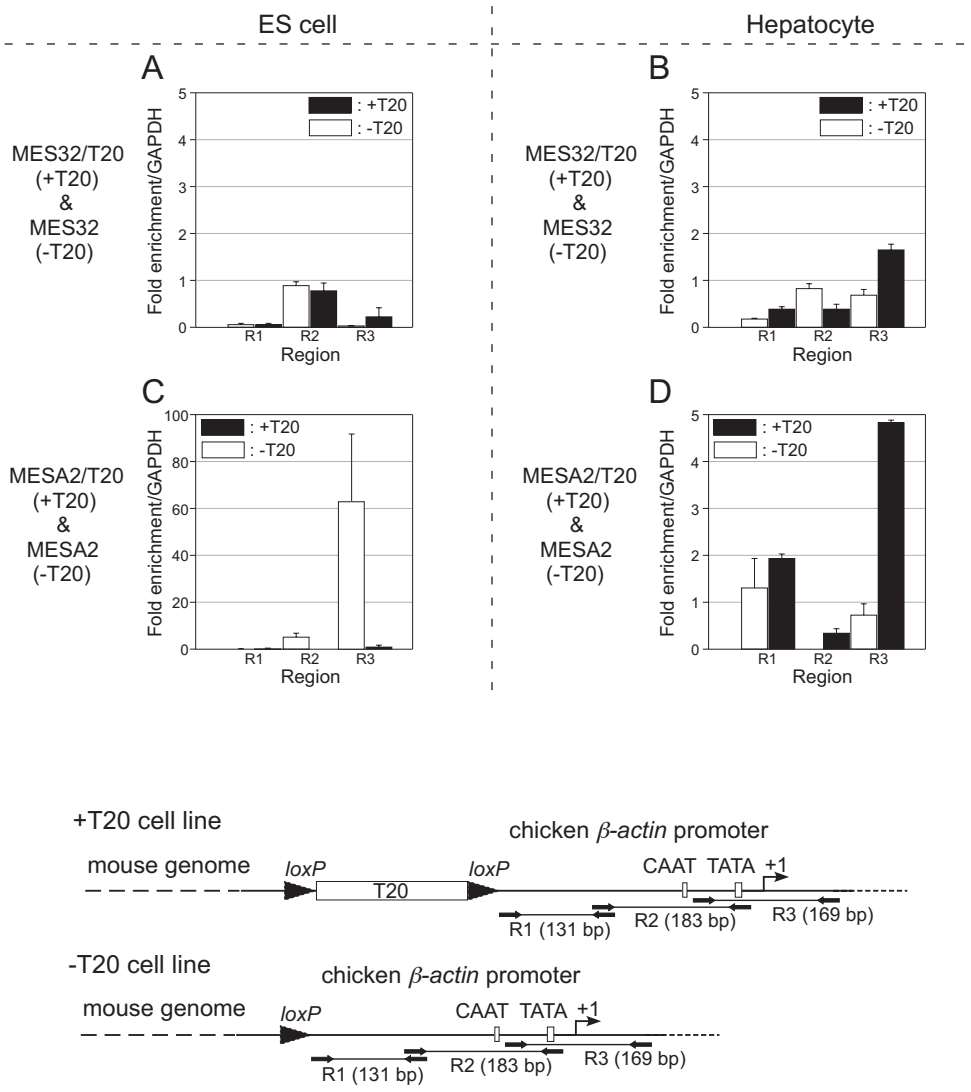

Fig. 10. Comparison of the distribution of histone H3 in T20-harboring and T20-less promoters

ChIP assays were performed using MES32/T20, MES32, MESA2/T20 and MESA2. The results for T20-less promoters are indicated with empty bars and those for T20-harboring promoters are indicated with filled bars. Values are shown as means ± SD (n = 3) of fold enrichment relative to the GAPDH gene. R1, R2 and R3 are the amplified regions and their locations are indicated at the bottom of the figure. Arrows indicate primer locations. +1 indicates the transcription start site.

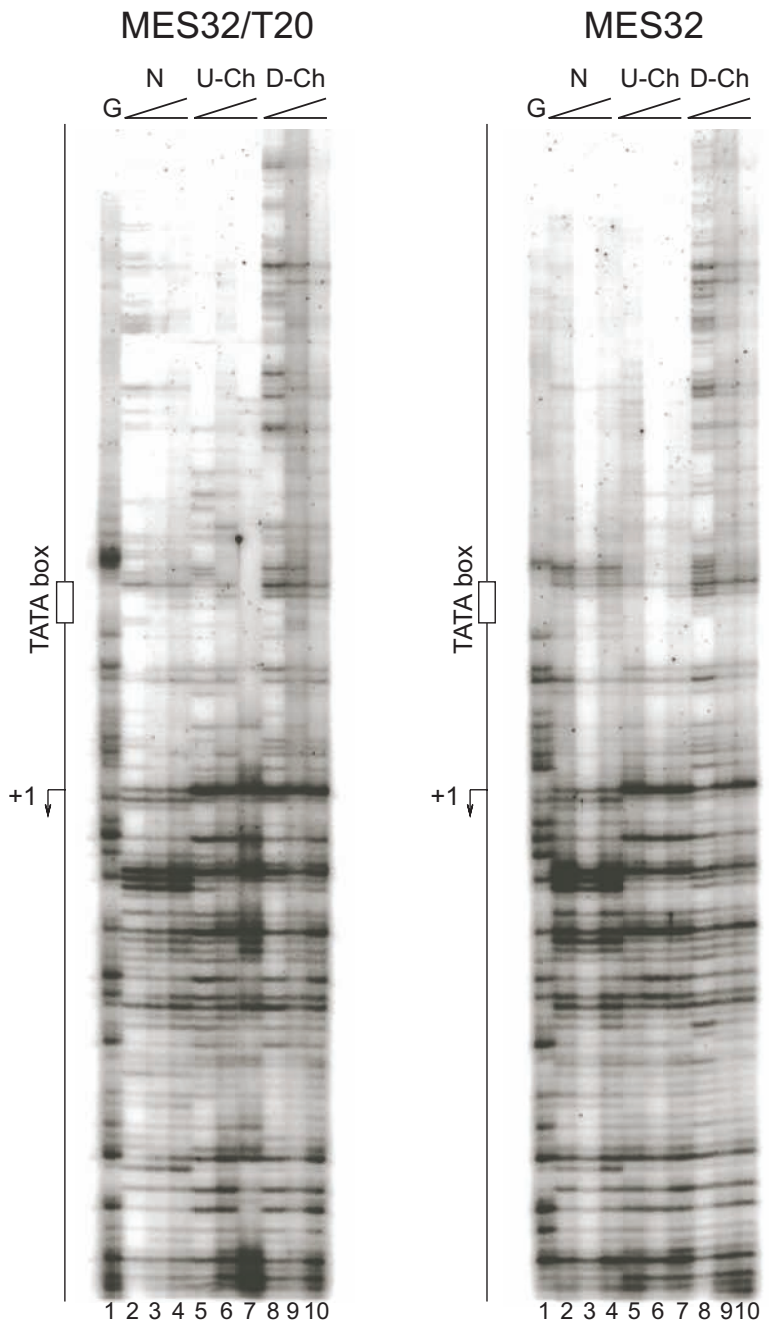

Fig. 11. DNase I sensitive sites in the promoter region of the reporter locus

The nuclei of the cell lines MES32/T20 and MES32 were isolated and treated with DNase I. Cleavage sites were detected by a combination of ligation-mediated PCR and primer extension. Lanes labeled N, U-Ch and D-Ch show DNase I cleavage sites in naked DNA, chromatin DNA from ES cells, and chromatin DNA from hepatocytes, respectively. G, G ladder; +1, transcription start site.

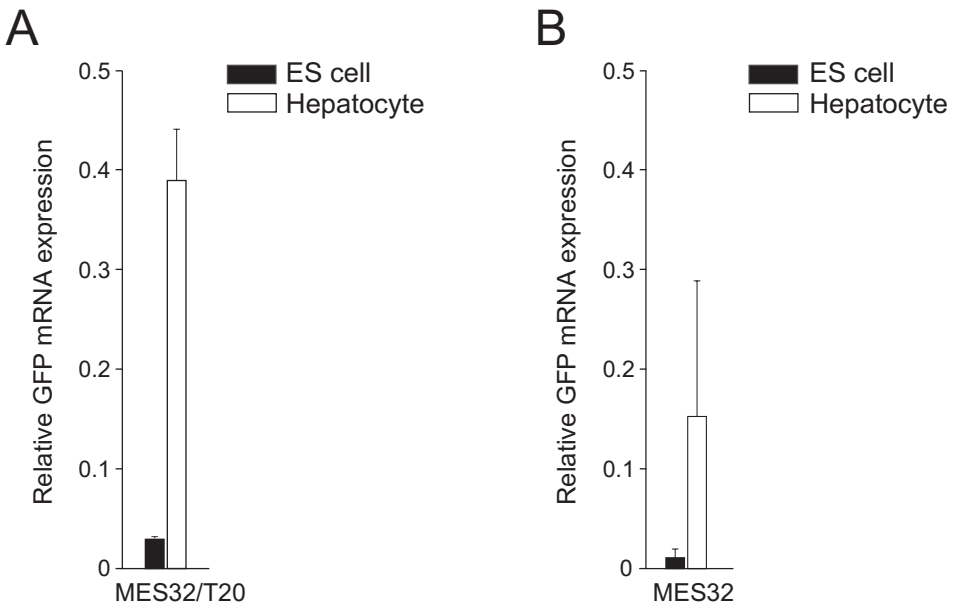

Fig. 12. Reporter gene expression in MES32/T20 and MES32 before or after cell differentiation

(A) Expression levels of reporter mRNA in MES32/T20 before (filled bar) and after (empty bar) cell differentiation. The expression level of Rps18 mRNA was used for normalization. Values are shown as means ± SD (n = 5).

(B) Expression levels of reporter mRNA in MES32 before (filled bar) and after (empty bar) cell differentiation. Values are shown as means ± SD (n = 5).

IV. Discussion

IV-1. Effect of T20 on transgene transcription before and after differentiation of mouse ES cells

The effect of T20 on transcription was seemingly small in mouse ES cells (maximum activation of 2.7-fold) and in hepatocytes differentiated from these cells (maximum activation of 2.5-fold) (Fig. 8). These results are in contrast to the previous data obtained in HeLa cells (maximum activation of about 90-fold) using the HSV *tk* promoter (Fig. 13) (61). However, the chicken *ß-actin* promoter used in the current work is a stronger promoter (83-85), and therefore the extent of activation of this promoter is not necessarily small. As an exogenous promoter, the chicken *ß-actin* promoter has been reported to be stronger than the simian virus 40 early promoter or Rous sarcoma virus long terminal repeat as assayed in mouse L cells (83). Furthermore, we found that the chicken *ß-actin* promoter was 10.4-fold stronger on average (n = 5) than the *tk* promoter in a transient transcription assay system using COS-7 cells (Fig. 14).

Down-regulation of transcription was also caused by T20 in some cell lines both before and after differentiation, which were seven cases in total (three before and four after differentiation). However, regarding group A cell lines, such phenomenon occurred only in MES25/T20 hepatocytes among six cases (three cell lines × two states). Furthermore, transcriptional decrease was slight in this case. Therefore, although regulation of gene expression is likely to be much stricter in ES cells and hepatocytes than in

HeLa cells, T20 seems to activate transcription generally when the reporter is integrated immediately upstream of a gene. This issue is further discussed below. The effect of T20 was also very large in COS-7 cells (61) in transient transfection assays, but this result cannot be compared directly with data in stable integrants.

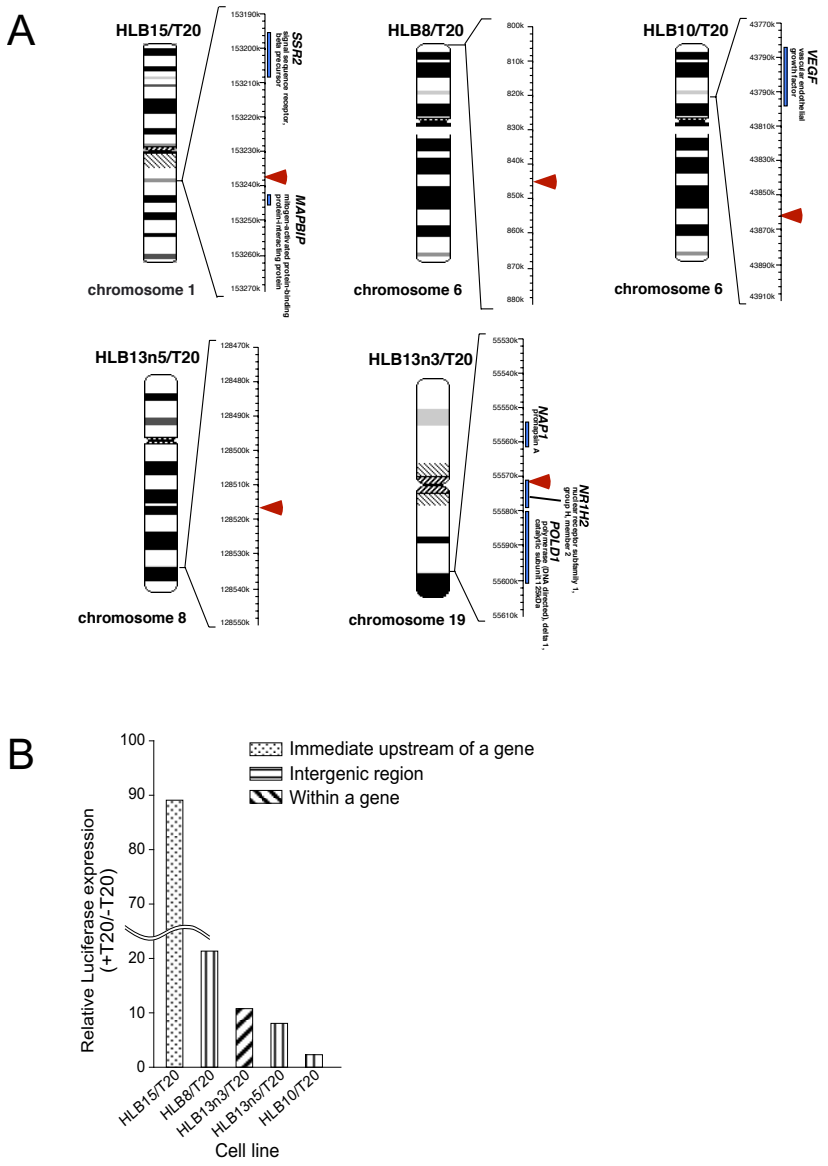

Fig. 13. Transgene loci in HeLa cell lines and the level of their expression

(A) Reporter loci. The loci of integration are indicated with arrowheads (Sumida *et al. FEBS J.* 2006). The corresponding normal human chromosomes are shown.

(B) Luciferase gene expression in each cell line. The relative luciferase expression (+T20/-T20) is calculated by dividing expression level of the luciferase gene (mean value) in each T20-harboring cell line by that in the corresponding control (T20-less) cell line.

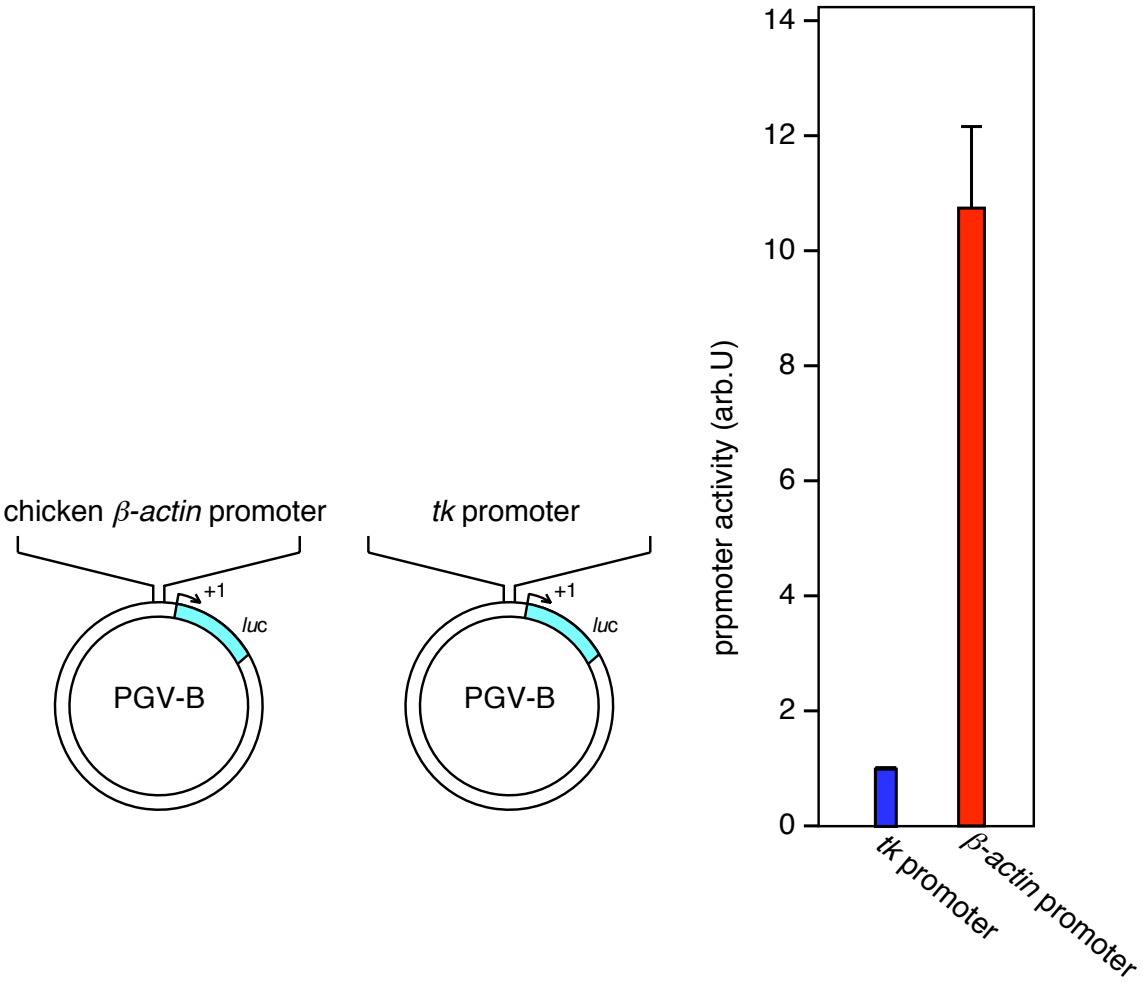

Fig. 14. Strength of the chicken *ß-actin* promoter as compared with that of the HSV *tk* promoter

The reporter plasmids were electroporated into COS-7 cells, and luciferase assay was carried out 21 hours after electroporation. The *ß-actin* promoter was 10.4-fold stronger than *tk* promoter.

IV-2. Reporter locus and T20 effect

Integration locus seems to have restricted the function of T20 in mouse ES cells and hepatocytes differentiated from these cells. In contrast, T20 did not exert any negative effect on transcription in HeLa cells irrespective of the integration locus (61). The highest activation by T20 in HeLa cells (90-fold) occurred when T20 was located immediately upstream of an active gene (Fig. 13). Thus, when T20 is integrated into transcriptionally active regions in chromatin, it may generally activate transcription even in the cells that have much stricter gene regulation system than HeLa cells. Indeed, for MES32/T20, in which the reporter was integrated upstream of *Tgfbr3*, which is expressed in both blastocysts and liver (87, 89), activation by T20 was maintained after differentiation (Fig. 8B). For MES7/T20, activation by T20 was also maintained in the hepatocytes, although the extent of activation decreased slightly. The neighboring gene in this case was *Cdk3*, which is active in ES cells (88) and in hepatocytes differentiated from the ES cells (Fig. 9). Therefore, these results are consistent with the speculative argument made above. However, activation did not occur in MES25/T20 hepatocytes (fold activation relative to the control was 0.87). Regarding MES25/T20, the neighboring gene (*Alox5ap*) is active not only in ES cells (86) but also in hepatocytes (Fig. 9). A drastic change in chromatin structure on and around the *Alox5ap* gene that was caused by cell differentiation may have had some negative structural influence on the reporter locus in this case.

It was indicated that similar chromatin structures were formed on T20-harboring and T20-less promoters in a transcriptionally active locus under the same state of differentiation (Figs. 10A, B, 11). In such a case, a "basic transcription" (transcription without the effect of T-20) may have occurred at the same level in each cell line in the same state of differentiation since the "shielding" effect by histones was similar in two cell lines. Therefore, in T20-harboring promoters, T20 should have determined the final levels of GFP mRNA expression.

The current study also suggests that chromatin structure formed on intergenic regions may not be strictly organized in ES cells and hepatocytes differentiated from these cells (Fig. 10C, D). This hypothesis is strengthened by the data that the effect of T20 was diverse in group B cell lines (Fig. 8). Thus, in the intergenic regions of mouse ES cells and hepatocytes, the main effector of reporter gene transcription was certainly histone deposition. The different chromatin structures on T20-harboring and T20-less promoters should produce different effects on transcription. However, we do not understand why the same locus forms different chromatin structures. The *loxP* sequence may be implicated in this phenomenon, since *loxP* has a palindromic sequence that can form a cruciform under unwinding stress (77 ,90). This cruciform is known to inhibit nucleosome formation (91, 92). Therefore, *loxP* may have influenced chromatin organization in different ways in some

T20-containing and T20-less promoters in intergenic regions. This effect, if any, may have been suppressed in transcriptionally active loci.

The rotational orientation of a curved DNA segment relative to the promoter and its distance from the promoter are important parameters for transcriptional activation (52, 61). However, these were not optimized in the current study, since to prepare control cell lines we had to use the Cre-*loxP* system. The *loxP* sequence of 34 bp between T20 and the *ß-actin* promoter was a hindrance for phasing and positional optimization of T20. Thus, it is probable that an appropriately positioned T20 will produce greater activation of transcription.

Chapter 2

Activation mechanism of chromatin transcription by superhelically curved DNA segments

V. Materials and methods

V-1. Plasmids and strains

A fragment containing the T20 segment was prepared by PCR from the plasmid pLHC20/*loxP*/TLN-6 as a template (61), using the set of primers, 5'-GCG GTA CCC TGG AGC GTC AGT CAG TTT TTC ATG-3' and 5'-GCG GTA CCC TCG AGG TTA TGA TAT CGG TGA AAA A-3'. The PCR fragment was digested with *Asp*718 and inserted into the *Kpn*I (*Asp*718) site of pKB112, the multicopy *CYC1-lacZ* plasmid (93). During the plasmid screening, those harboring a T12 or T28 segment at the same site were also obtained. The plasmids were digested with *Xho*I to delete the UAS region from the *CYC1* promoter, to construct pTM6-U11-5 (T12), pTM44-U4-5 (T20) and pTM67-U8-15 (T28). All of the plasmids thus obtained were verified by DNA sequencing. The plasmid pLGΔ312ΔSS (94), in which the UAS region was deleted from the *CYC1-lacZ* gene, was used as a control plasmid. These plasmids were introduced into *S. cerevisiae* strain AMP105 [*MATa ho::LYS2 ura3 lys2 leu2::hisG*].

V-2. β-galactosidase assay

The β -galactosidase assay was performed with early exponential phase cells grown in SC-Ura medium. The assay was carried out according to the standard protocol (95) with a minor modification: Y-PER (Pierce Chemical, Rockford, IL, USA) was used to prepare permeabilized yeast cells, instead of chloroform. The assay results were the average of three independent cultures of each strain.

V-3. MNase digestion-based analysis of chromatin structure

Yeast cells harboring plasmids were cultured in SC-Ura medium until OD_{600} reached ~1.0. Nuclei were isolated and micrococcal nuclease (MNase) digestion was performed as described previously (96). The cleavage-sites for MNase were analyzed by indirect end-labeling, as described previously (97). Samples were digested with *Stu*I, which cut at +442 (translation start site of *URA3* gene is +1) of the *URA3* gene in the plasmids. The products were separated on a 1.5% agarose gel prepared in 1×TBE buffer, transferred onto a Hybond-XL membrane (GE-Healthcare, Little Chalfont,UK), and detected by a radioactively labeled probe (201 bp) corresponding to the region from +442 to +642 in the *URA3* gene. The nucleosome repeat assay was performed as described (97). The MNase digested samples were separated on a 1.3% agarose gel, transferred onto the Hybond-XL membrane, and detected by radioactively-labeled probes corresponding to the region of the *CYC1* promoter, the T12, T20, or T28 segments, and the *URA3* region. The probe for the promoter was prepared by using primers 5'-ATG GCC AGG CAA CTT TAG T-3' and 5'-GCT ACA AAG GAC CTA ATG TAT AAG GAA-3'. The primer sets used to prepare the other probes are described in the ChIP assay section.

V-4. DNase I footprinting assay

Aliquots (200 μl) of the nuclear suspension were incubated at 37°C for 1 min. Then, 0.01 U, 0.1 U or 1 U of DNase I was added, and digestion was performed at 37°C for 2 min. Naked DNA was digested with 0.0001 U, 0.002 U or 0.003 U of DNase I at 37°C for 2 min. After digestion, the products were purified and dissolved in water. The DNase I cleavage sites were detected by PCR-based primer extension (52), using a [5'-^{32}P]-labeled primer 5'-AGT GAG ACG GGC AAC AGC-3' (to detect the cleavage sites in the promoter region) or 5'-CAC ATG CAT GCC ATA TGA T-3' (to detect the cleavage sites in the upstream region of the promoter) under the following conditions: 95°C for 5 min and 35 cycles at 95°C for 30 sec, 63°C for 15 sec and 72°C for 2 min. All samples were purified and resolved in 6% polyacrylamide-7 M urea gels.

V-5. ChIP assay

The ChIP assay was performed according to Kuo and Allis (98) with slight modifications. To obtain the chromatin fragment, the cell lysate was digested with 20 U of MNase at 37°C for 20 min. After cell debris was removed, 60 μl of the lysate was used for immunoprecipitation and subsequent DNA purification, which was performed in triplicate with a OneDay ChIP Kit (Diagenode, Liège, Belgium) according to the manufacturer's instructions, using antibodies against histone H3 (ab1791; Abcam, Cambridge, UK). Using 2 μl of the DNA samples, quantification of fragments containing a part of the nucleosome I, II or II' DNA was performed by SYBR Green quantitative real-time PCR with the StepOne Plus real-time PCR system and StepOne software v. 2.1. Quantification of fragments containing part of the nucleosome III DNA was carried out simultaneously as an internal control. The primer sets were as follows: for the nucleosome I region, 5'-GTG TGC GAC GAC ACT GAT-3' and 5'-AGA GAA AAG AAG AAA ACA AGA GTT-3'; for the nucleosome II region, 5'-GGC TGG GAA GCA TAT TTG AG-3' and 5'-TTG AAG CTC TAA TTT GTG AGT TTA GT-3'; for the nucleosome II' region, 5'-TGG TAC CCT GGA GAG TAG TCA G-3' and 5'-CGG ATC TGC TCG AGG TTA TG-3'; for the nucleosome III region, 5'-AGA ACC GTG GAT GAT GTG GT-3' and 5'-CCT TCC CTT TGC AAA TAG TCC-3'. The relative sample enrichment was calculated using the formula: $2^{-(Ct\ target\ region-Ct\ nucleosome\ III\ region)}$

VI. Results

VI-1. Effect of superhelically curved DNA on transcription in yeast

When the UAS region is deleted from the *CYC1* promoter in a *CYC1-lacZ* plasmid, the remaining downstream promoters are activated by nucleosome depletion (99). This implies that the promoter activity is responsible for the nucleosome occupancy in this system. We chose it to examine mechanisms of transcriptional activation by superhelically curved DNA structures, for we assumed that the activation would be mediated by chromatin alteration. The UAS-deleted yeast *cytochrome c* (*CYC1*) promoter is known to be a "nucleosome-responsive" promoter, which was activated 94-fold by nucleosome depletion (99). The superhelically curved DNA segments T12, T20 and T28 were introduced into the UAS-deleted *CYC1* promoter (Fig. 15), and their effects on transcription were examined by measuring the β-galactosidase activity. As shown in Fig. 16, all of the curved DNA segments activated transcription, and the observed fold activations relative to the control were 51.4 (T12), 63.4 (T20) and 56.4 (T28), respectively. Thus, superhelically curved DNAs can activate transcription not only in mammalian cells but also in yeast cells. Furthermore, the extents of activation by these segments were comparable to those induced by the nucleosome-free effect described above.

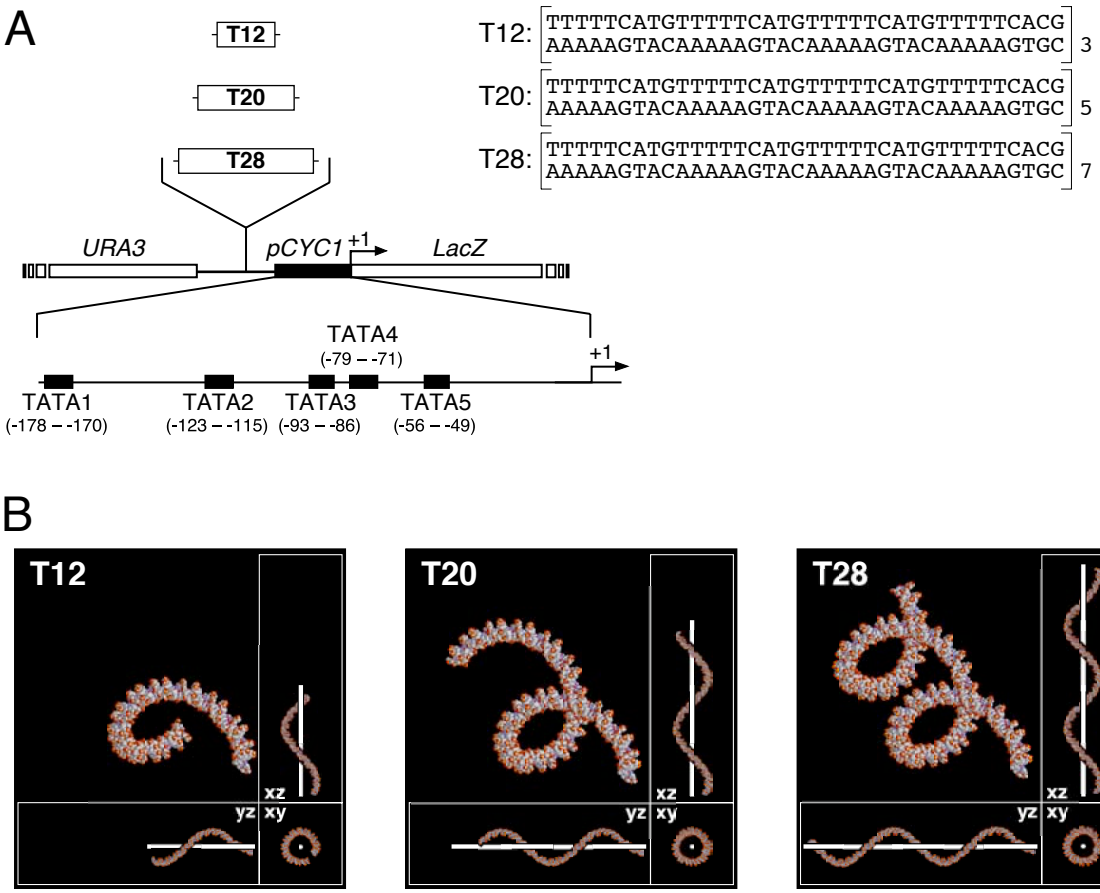

Fig. 15. Reporter constructs used in this study and architecture of superhelically curved DNAs

(A) Reporter constructs. "*pCYC1*", "+1" and "TATA" indicate *CYC1* promoter, translation start site and TATA box, respectively. The *CYC1* promoter contains five TATA sequences, and they were distinguished by the numbering according to the report by Li and Sherman (106). The nucleotide sequence of T20 is slightly different from that in the previous report (61): the sequence started with 5'-TCAGTTTTT and ended with TTTTT-3' in the previous T20, but the corresponding sequences are TTTTT and TTTTTCACG-3' in the present T20. However, since they have the same three-dimensional architecture, the same name was used for convenience. (B) Three-dimensional architectures of T12, T20 and T28. They were drawn as reported previously (61). The white line indicates the superhelical axis.

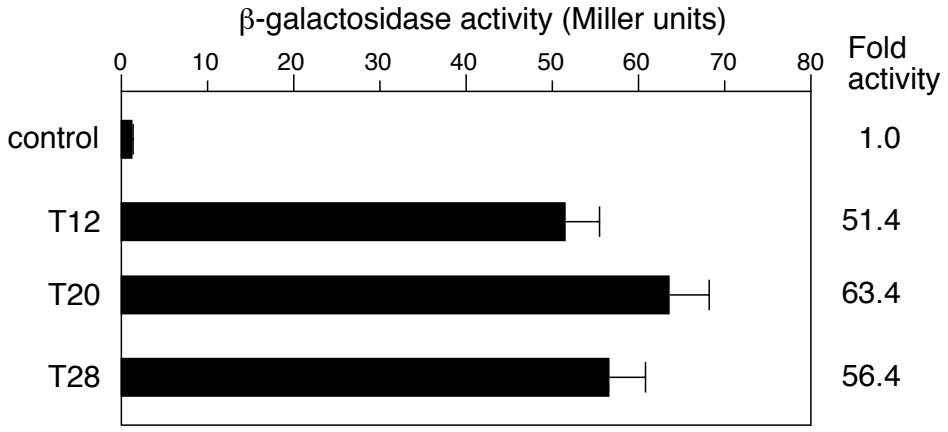

Fig. 16. Effect of superhelically curved DNA on transcription

The promoter activity was determined in a ß-galactosidase assay. Values shown are means ± SD (n = 3).

VI-2. Positioning of nucleosomes on and around the promoter

To determine how T12, T20 and T28 activated transcription, at first, the potential sequence-specific localization (translational positioning) of the nucleosomes on the region containing a curved DNA and the *CYC1* promoter was investigated by an indirect end-labeling analysis (Fig. 17) (97, 100-105). Plasmid-containing nuclei were isolated, and were subjected to digestion with micrococcal nuclease (MNase), and subsequently to the analysis (Fig. 18). The bands shown with white arrowheads indicate the sites that were digested by the enzyme in the naked state, but were fully or partially protected in chromatin. On the other hand, the bands shown with black arrowheads indicate the sites that were newly or highly digested in chromatin. Based on these signal profiles and the distances between the black arrowheads, the nucleosome positions were deduced.

Regarding the chromatin formed on the control construct ("control chromatin"), three nucleosomes, referred to as I, II and III, were suggested to be present as indicated in the figure: the latter two were located upstream of the TATA1 sequence and the first one was on the promoter. Nucleosomes I and III also seemed to lie on the corresponding regions in the curved DNA-harboring each construct. In the control chromatin, nucleosome I was deduced to be located between -40 and -190 relative to the translation start site, and the distance between these positions was 150 bp, while in each chromatin formed on the curved DNA-containing construct (referred to below as T12, T20 or T28 chromatin, or together as

Tn chromatin), it was presumably located between -40 and -240, and the distance between them was 200 bp. Therefore, nucleosome I seemed to cover a wider region in the Tn chromatin. The presence of a nucleosome (referred to as nucleosome II') on the T12, T20, or T28 region was also speculated. In the locus of nucleosome II', we detected several sites that were slightly but obviously digested in the chromatin, as indicated with black arrowheads in parentheses. They seemed to indicate the edges of nucleosomes with different translational positions. Furthermore, another nucleosome might be located between nucleosomes II' and III, as indicated by the dashed ellipse in the figure.

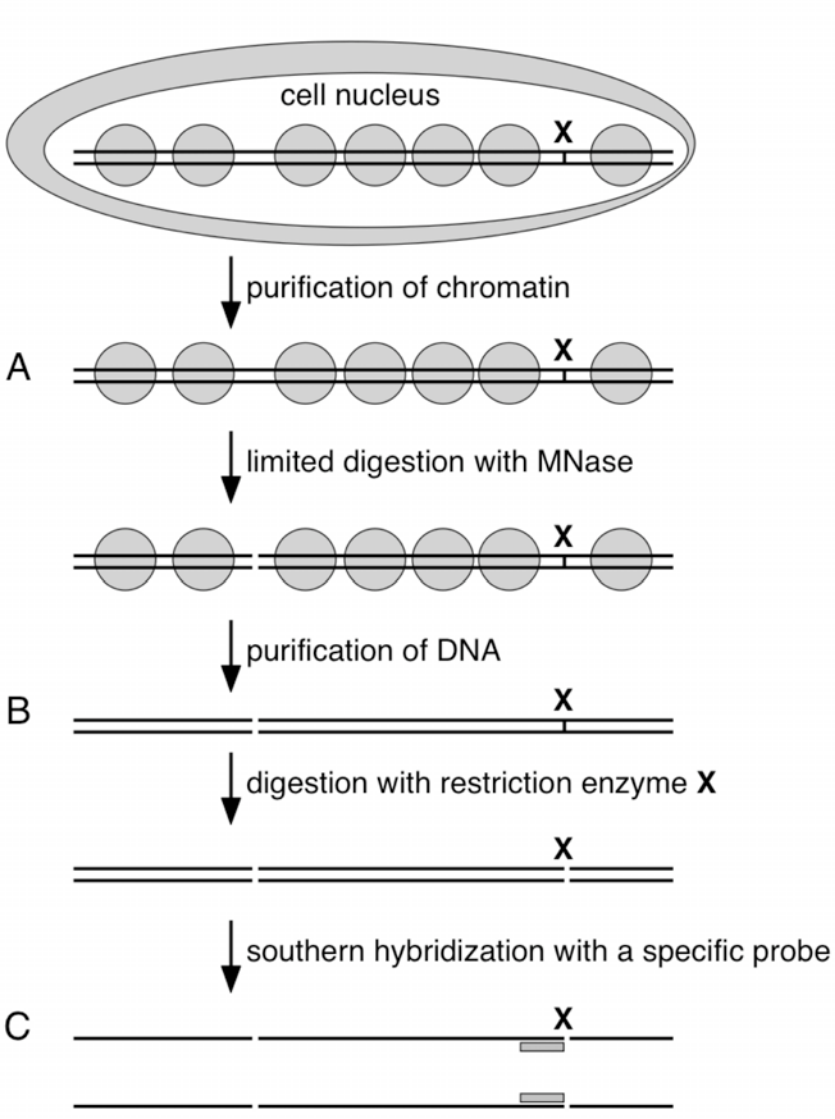

Fig. 17. Procedure for mapping of nucleosome cleavage sites by indirect end-labeling

(A) Chromatin is partially digested with MNase and purified. (B) DNA is digested with restriction enzyme X. (C) The products are electrophoresed on an agarose gel and subjected to Southern blot analysis with a specific probe, and the MNase cleavage site is identified by corresponding band size and its distance from the restriction site X.

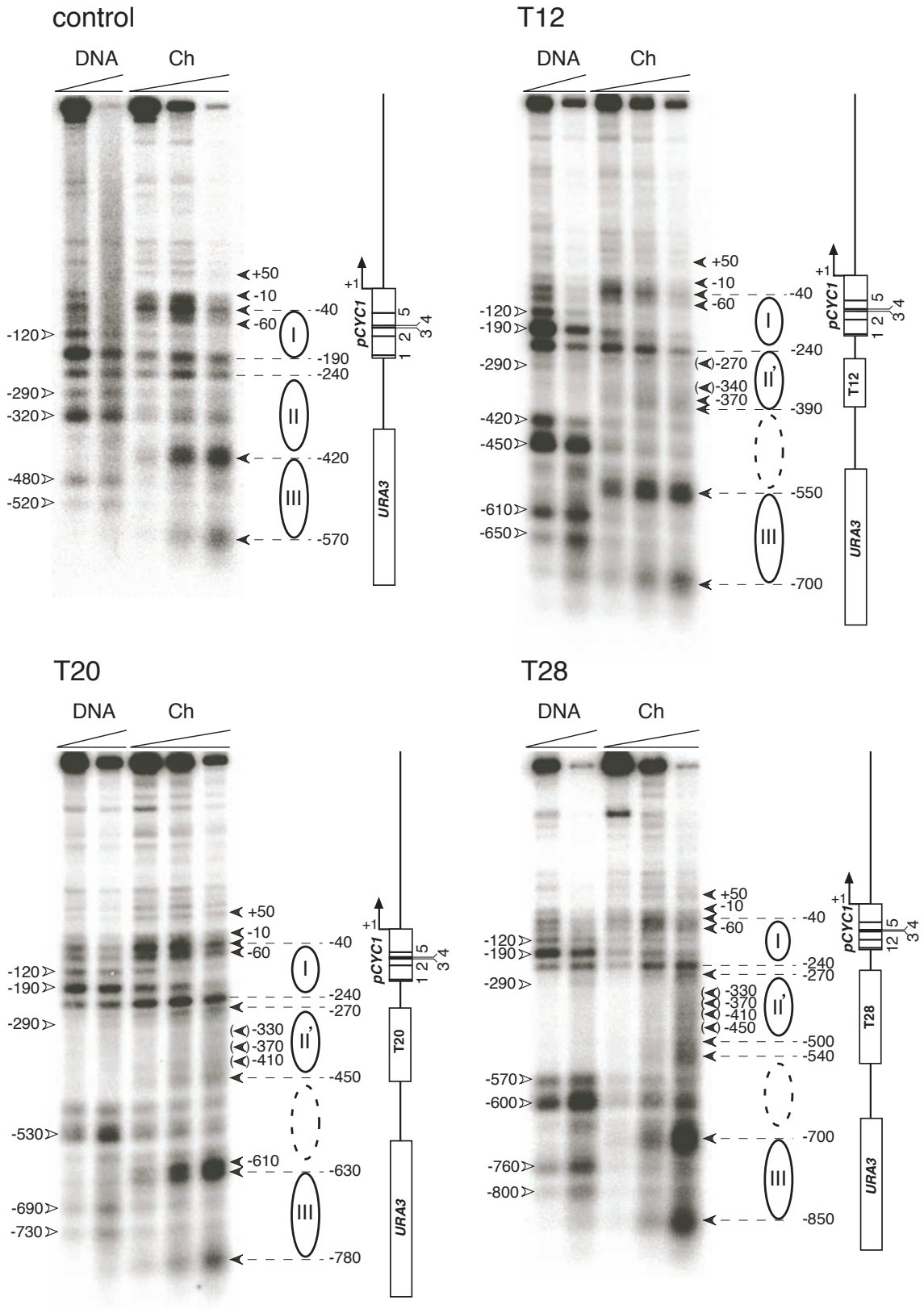
control
DNA
Ch
-120
-290
-320
-480
-520
+50
-10
-60
-40
-190
-240
-420
-570
I
II
III
+1
pCYC1
1 2 5
3 4
URA3
T12
-120
-190
-290
-420
-450
-610
-650
+50
-10
-60
-40
-270
-340
-370
-240
-390
-550
-700
II'
T20
-120
-190
-290
-530
-690
-730
-330
-370
-410
-450
-610
-630
-780
T28
-120
-190
-290
-570
-600
-760
-800
-500
-540
-700
-850

Fig. 18. Analysis of translational positions of nucleosomes on the upstream region of the reporter gene

The upstream structure of the translation start site is illustrated on the right side of each gel. The lines with a number in the *CYC1* promoter (*pCYC1*) indicate the five TATA sequences. In each set of data, the lanes labeled Ch indicate the MNase digestion of isolated nuclei (chromatin) at three nuclease levels, and the lanes labeled DNA indicate the MNase digestion of the naked DNA at two nuclease levels, as a control. Arrowheads indicate the following sites: white, fully or partially protected in chromatin; black, highly digested or specifically digested in chromatin; parenthesized black, digested more in chromatin than in naked DNA, but the digestion itself was slight. Position numbers are relative to the translation start site (+1). The ellipses with I, II, II' or III indicate putative nucleosomes, as deduced from the band patterns. Dashed-lined ellipses: possible additional positions.

VI-3. Confirmation of the nucleosome presence

To determine whether nucleosomes I, II, II' and III were actually formed on the regions indicated in Fig. 18, the chromatin digests with MNase were subjected to a Southern blot analysis, using probes prepared from the relevant regions. As shown in Fig. 19, so-called "nucleosomal ladder" patterns were detected by all of the probes, which supported the presence of the putative nucleosomes indicated in Fig. 18. However, the curved DNA probes *c*, *d* and *e* hardly detected DNA fragments of mononucleosome size, but detected fragments with sizes between mono- and dinucleosomal DNAs, which appeared as smeared bands between these two positions. This pattern was not observed when the other probes were used. These smeared patterns could be a consequence of the difficulty in digesting the curved DNA regions, as shown in Fig. 18. In addition, it is possible that nucleosome II' had multiple translational positionings, as described in the previous section. In such a case, the outside regions of each curved DNA could be protected from MNase digestion by the positioned histone cores. These two factors could generate DNA fragments longer than that of mononucleosomal DNA.

The relative populations of the nucleosome-forming constructs were analyzed by a ChIP assay. The immunoprecipitation was performed using the antibody against histone H3. The population of nucleosome III was used as a reference for comparison (Fig. 20). The relative populations of nucleosome I to nucleosome III were 61% for the control construct, 69%

for the T12-harboring construct ("T12 construct"), 43% for the T20 construct and 85% for the T28 construct. Except for the T20 construct, the curved DNA-flanked promoter resulted in a more nucleosome formation than the curved DNA-less (control) promoter, while the promoter activity of the former was much higher (more than 50-fold). Obviously, the transcription data in Fig. 16 could not be explained in terms of the extent of histone deposition. Furthermore, these data showed that transcription was highly activated, even from the nucleosome harboring promoter.

The promoter proximal nucleosomes were nucleosomes II and II'. The populations of nucleosome II' gradually increased, according to the greater length of the curved DNA region. Regarding nucleosomes II and II', the control construct and the T28 construct had comparable populations. However, T28 activated the promoter by more than 50-fold. Therefore, the presence of nucleosomes II and II' themselves was not implicated in determining the transcription level.

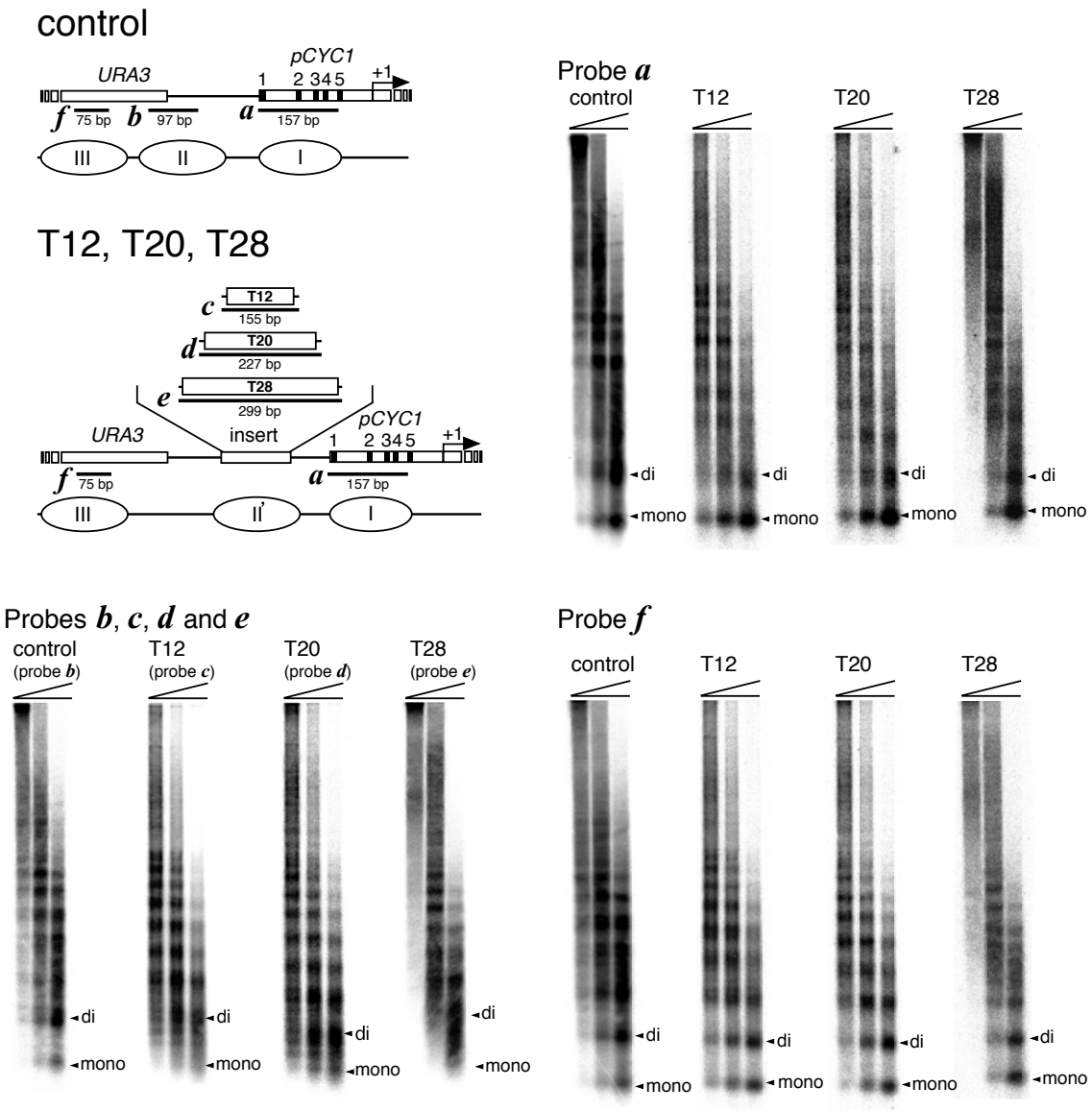

Fig. 19. Southern blot analysis of DNA fragments obtained from MNase digests of nuclei

The digestion products were hybridized with probes obtained from the promoter (probe ***a***), the curved DNA regions (probes ***c***, ***d*** and ***e***), the *URA3* region (probe ***f***) or the region between the promoter and the *URA3* region in the control construct (probe ***b***). The positions and lengths of these probes are illustrated. Black boxes in the *CYC1* promoter indicate the TATA sequences 1 to 5. Nucleosomes are shown as ellipses with Roman numerals. The MNase digestion of isolated nuclei (chromatin) was performed at three nuclease levels. 'mono' and 'di' indicate mono- and dinucleosomes, respectively.

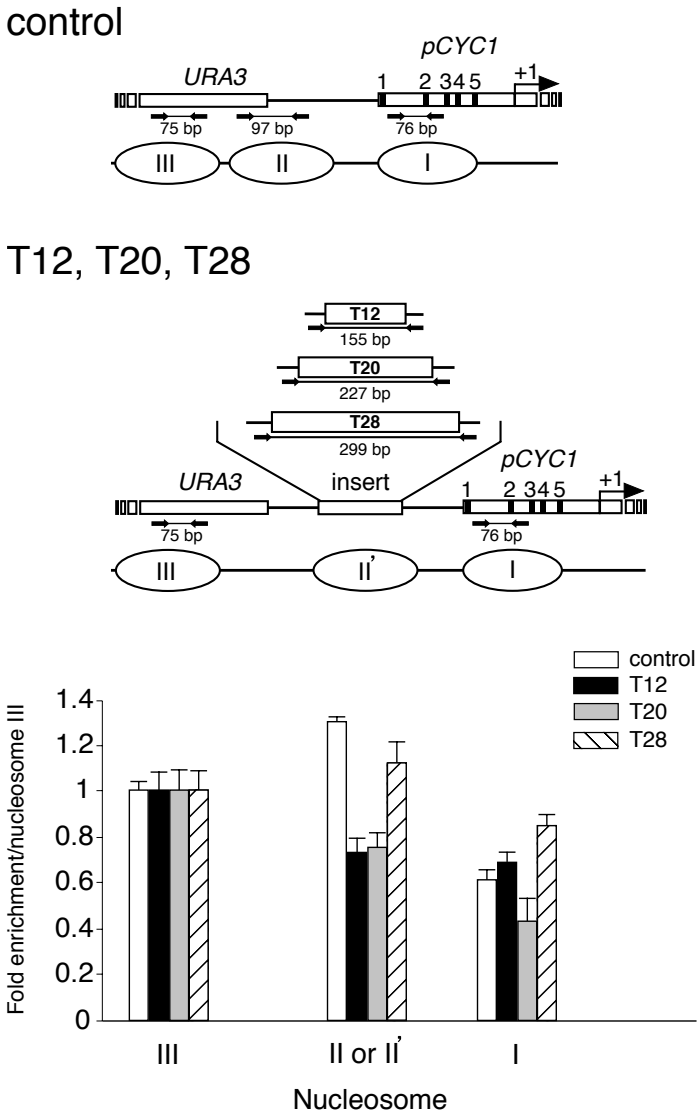

Fig. 20. Relative populations of nucleosomes I, II, II' and III, as determined by a ChIP assay

The assay was performed using the antibodies against histone H3. In the schematic drawing, the amplified regions and their locations are indicated with lines, with arrows indicating PCR primers. In the histogram, the fold enrichment of each nucleosome relative to nucleosome III is indicated with different bars: white, control chromatin; black, T12 chromatin; gray, T20 chromatin; striped, T28 chromatin (means ± SD of three determinations).

VI-4. Accessibility of DNA in chromatin

We subjected the same nuclear fraction to DNaseI digestion (52) to investigate the accessibility of the DNA in chromatin in order to understand how curved DNAs could activate transcription. The control construct and the curved DNA-containing constructs share the same sequence, except for the curved DNA region (Fig. 15). In the region with the same sequence, a notable difference was only detected within the TATA3 sequence (Figs. 21-25). In the control construct, A_{-92} and A_{-91} were highly accessible in the naked DNA, and their accessibility was maintained even in chromatin. On the other hand, the sites with high accessibility were shifted by one nucleotide toward the center of the TATA3 sequence in the curved DNA-containing constructs in the naked states. As a result, A_{-91} and A_{-90} became highly accessible.

The accessibility of these two sites was maintained in the T20 chromatin. In addition, as in the case of the control chromatin, A_{-92} was also accessible in this chromatin. Although the cleavage signal at A_{-90} was less marked in the T12 chromatin and the T28 chromatin, as compared with that in the T20 chromatin, the signal definitely existed (see lane 9 in each panel). In conclusion, the exposed sequence was shifted towards the center of the TATA3 sequence in the curved DNA-containing constructs in the naked DNA, and this exposure was maintained even in chromatin. Since the distance between -240 and -90 is 150 bp (Fig. 18), position -90 seemed to be the downstream end of a certain population of nucleosome I.

Regarding the curved DNA region, interestingly, both the positions and intensities of the cleavage signals were almost the same between naked DNA and chromatin in each Tn chromatin. Clear “10 bp ladder” cleavage patterns with a rung spacing of 9 bp were observed, indicating that the rotational setting of the DNA was maintained even in the chromatin (Figs 22, 23, 24).

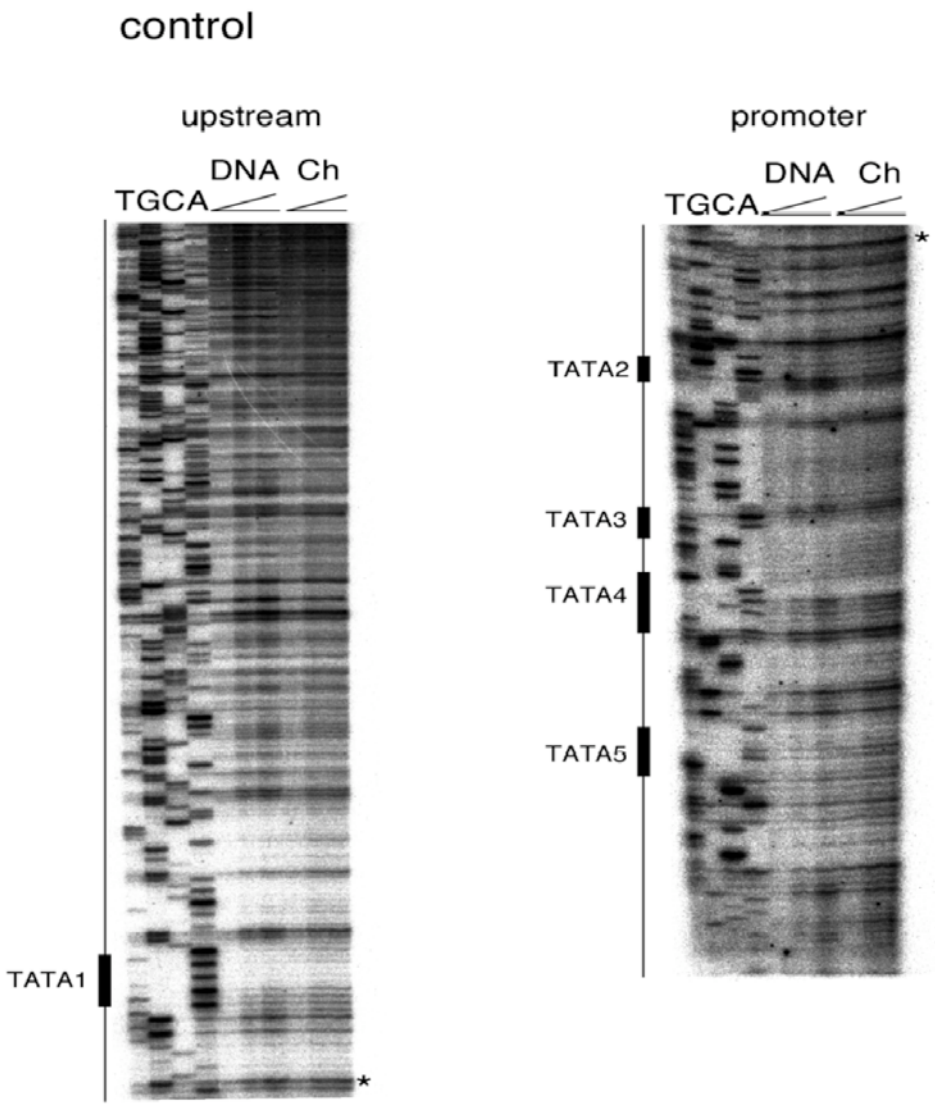

Fig. 21. Accessibility of DNA in chromatin

Nuclei harboring control construct were digested with DNase I, and the cleavage sites were analyzed as described in the Materials and Methods. 'DNA' and 'Ch' indicate DNase I cleavage sites in naked DNA and chromatin, respectively. The black arrowheads indicate the "10 bp ladder" (the rung spacing is 9 bp). The asterisk on the right of each autoradiogram indicates overlap points of the signals.

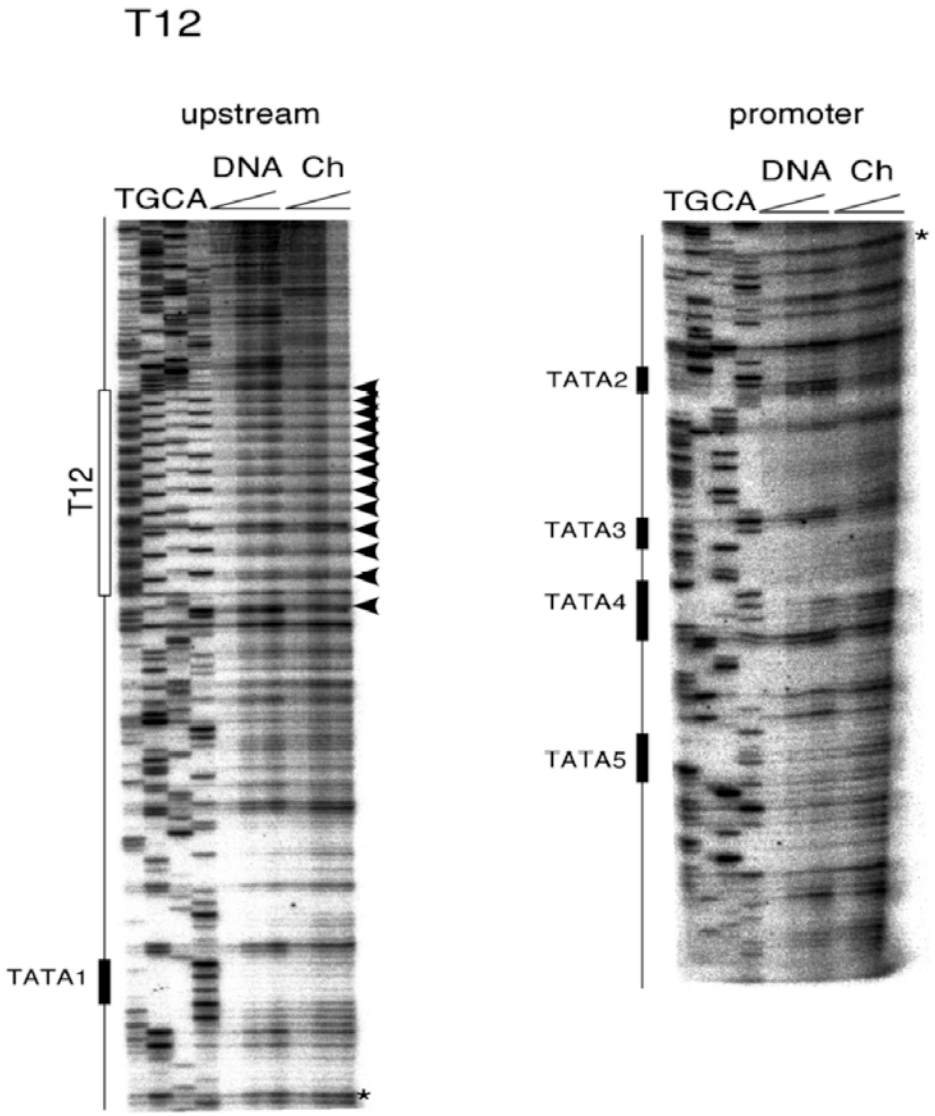

Fig. 22. Accessibility of DNA in chromatin

Nuclei harboring T12 construct were digested with DNase I, and the cleavage sites were analyzed as described in the Materials and Methods. 'DNA' and 'Ch' indicate DNase I cleavage sites in naked DNA and chromatin, respectively. The black arrowheads indicate the "10 bp ladder" (the rung spacing is 9 bp). The asterisk on the right of each autoradiogram indicates overlap points of the signals.

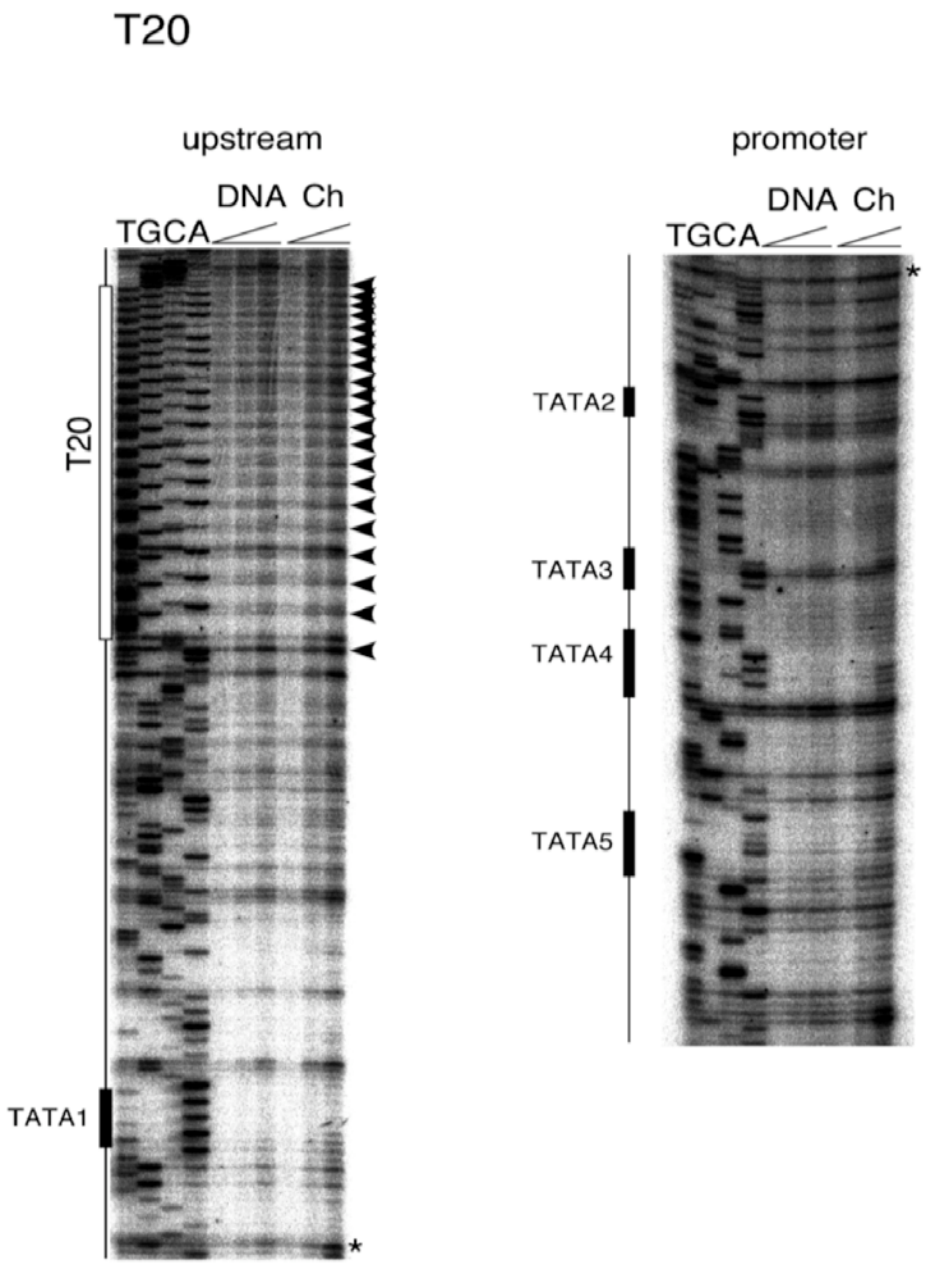

Fig. 23. Accessibility of DNA in chromatin

Nuclei harboring T20 construct were digested with DNase I, and the cleavage sites were analyzed as described in the Materials and Methods. 'DNA' and 'Ch' indicate DNase I cleavage sites in naked DNA and chromatin, respectively. The black arrowheads indicate the "10 bp ladder" (the rung spacing is 9 bp). The asterisk on the right of each autoradiogram indicates overlap points of the signals.

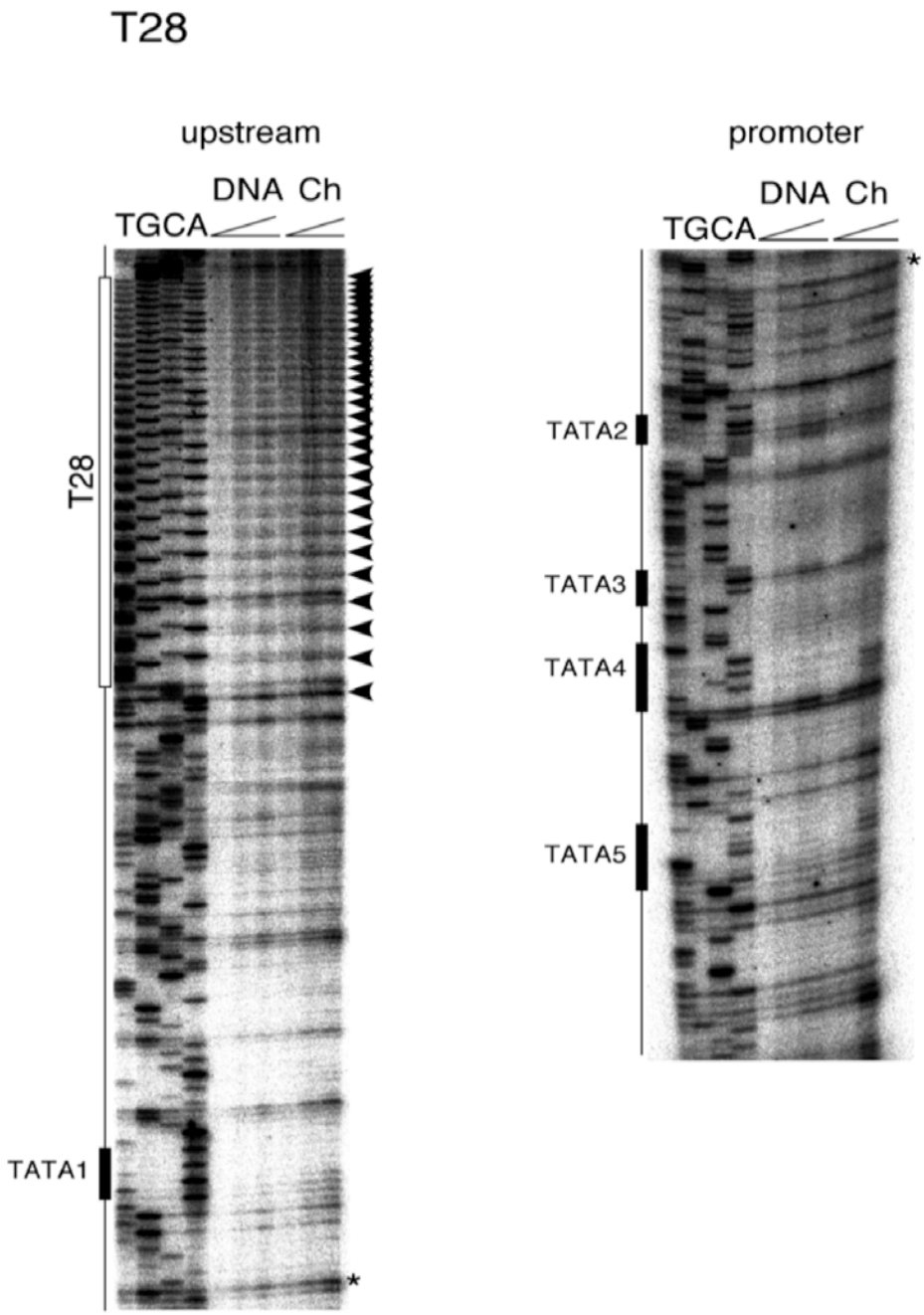

Fig. 24. Accessibility of DNA in chromatin

Nuclei harboring T28 construct were digested with DNase I, and the cleavage sites were analyzed as described in the Materials and Methods. 'DNA' and 'Ch' indicate DNase I cleavage sites in naked DNA and chromatin, respectively. The black arrowheads indicate the "10 bp ladder" (the rung spacing is 9 bp). The asterisk on the right of each autoradiogram indicates overlap points of the signals.

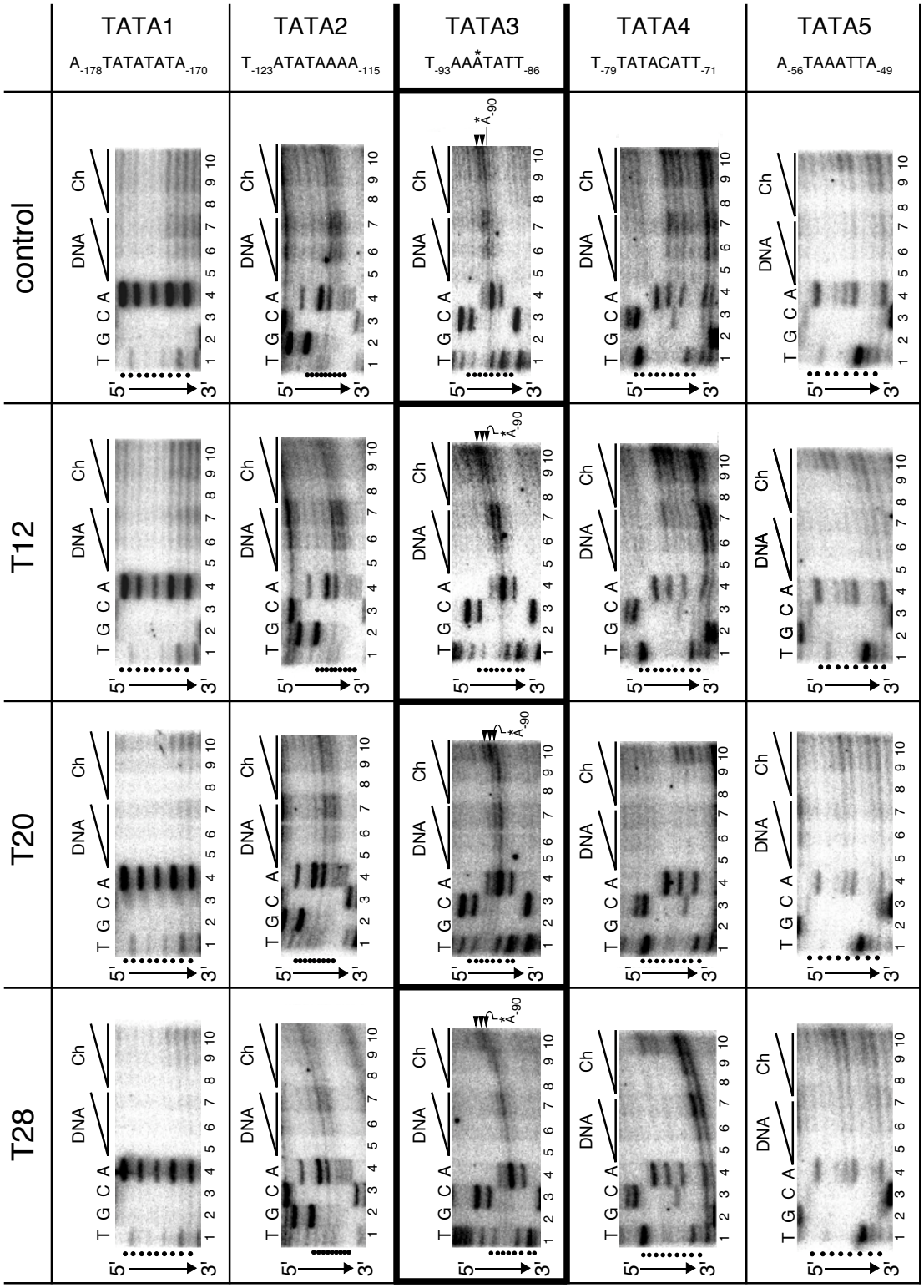

Fig. 25. Accessibility of DNA in chromatin

Nuclei harboring each construct were digested with DNase I, and the cleavage sites were analyzed as described in the Materials and Methods. 'DNA' and 'Ch' indicate DNase I cleavage sites in naked DNA and chromatin, respectively. The dots on the left-hand side of each gel indicate the positions of TATA-comprising nucleotides. Highly digested nucleotides within the TATA3 sequence in the chromatin are indicated with black arrowheads, and the position of A_{-90} is also indicated.

VII. Discussion

Using a yeast minichromosome system, the present study investigated why superhelically curved DNA segments can activate transcription in chromatin. Chromatin analyses confirmed that the major populations of the reporter constructs formed nucleosomes on the *CYC1* promoter, the curved DNA region and the *URA3* region. Regarding the promoter region, there were two clear differences between the control chromatin and the Tn chromatin. One was that nucleosome I was located between -40 and -190 in the control chromatin, while it was located between -40 and -240 in the Tn chromatin (Fig. 18). The other was that the center region of the TATA3 sequence was more exposed in the Tn chromatin than in the control chromatin (Fig. 25). Previous reports described that the TATA1 and TATA2 sequences were responsible for transcription from the *CYC1* promoter (106, 107). However, considering that the extent of exposure of these sequences in the Tn chromatin was almost the same as that in the control chromatin (Fig. 25) and that the transcription from the *CYC1* promoter is repressed in the presence of nucleosomes (99), the TATA3 sequence was presumably responsible for the transcription of the reporter gene in the present case.

If the upstream edge of nucleosome I was -240 in the Tn chromatin, then the downstream edge should have been located around -90, which is the center region of the TATA3 sequence. A certain population of chromatin seemed to adopt this positioning, since -190 was considerably

protected against the digestion (Fig. 18). However, considering that the locus of nucleosome I (the protected region) spanned from -40 to -240, different translational positions were also presumably adopted by the other populations. The increased mobility of nucleosome I in the Tn chromatin seems to have generated the wide signal for the translational positioning. Under this condition, the TATA3-exposing population of the nucleosome I was generated, and it was presumably implicated in the transcriptional activation in the Tn chromatin. A quite similar result was obtained in the system using a short, left handedly curved DNA segment, T4. When T4 (36 bp) was linked to the HSV *tk* promoter at a specific rotational phase and distance, it attracted the histone core and the TATA box was thus left in the linker DNA with its minor groove facing outwards, which led to the activation of transcription (52). However, the activation by T4 was approximately 10-fold. Thus, to explain the activation by more than 50-fold, an additional parameter still seems to be necessary. It may be the sliding ability of nucleosome II', which would also explain the increased mobility of nucleosome I.

Nucleosome II' seemed to have multiple translational positions, while, in contrast, the position of nucleosome II was almost fixed (Figs. 18 and 19). This difference was obviously caused by the underlying DNA, and the superhelically curved DNAs were certainly implicated in the multiple positioning of nucleosome II'. It is known that curved DNA structures favor nucleosome formation (109-112). Therefore, the wide-ranging DNA

curvature is likely to have the ability to slide the histone core. This hypothesis is supported by the report that nucleosome sliding is a general phenomenon that is dependent on the underlying DNA sequence (113). Furthermore, nucleosome sliding is considered as an important way of regulating access to DNA sites that are near nucleosome borders (114). The data shown in Figs. 18 and 19 strongly suggest that the sliding of nucleosome II' indeed occurred in the curved DNA region. The high mobility of the histone core seems to have increased the mobility of nucleosome II'. Furthermore, it must also be noted that TBP binding to DNA can induce nucleosome sliding (115). Therefore, we can envision a scenario in which the high mobility of nucleosome II' enables nucleosome I to fluctuate. This fluctuation enhanced the chance of TBP binding to the TATA3 sequence, which then induced further sliding of these nucleosomes transiently, and the resulting open structure highly facilitated transcription initiation (Fig. 26). Although the dynamic features of these events could not be detected in our "static analyses", it is quite possible that a superhelically curved DNA segment could function as an acceptor of the sliding histone core and assist the dynamic process of transcription.

The rotational orientation and the distance of a curved DNA segment relative to the promoter are important parameters for transcriptional activation (52, 61). However, these were not optimized in the present study. Therefore, further positional refinement of each segment might have produced even greater transcriptional activation.

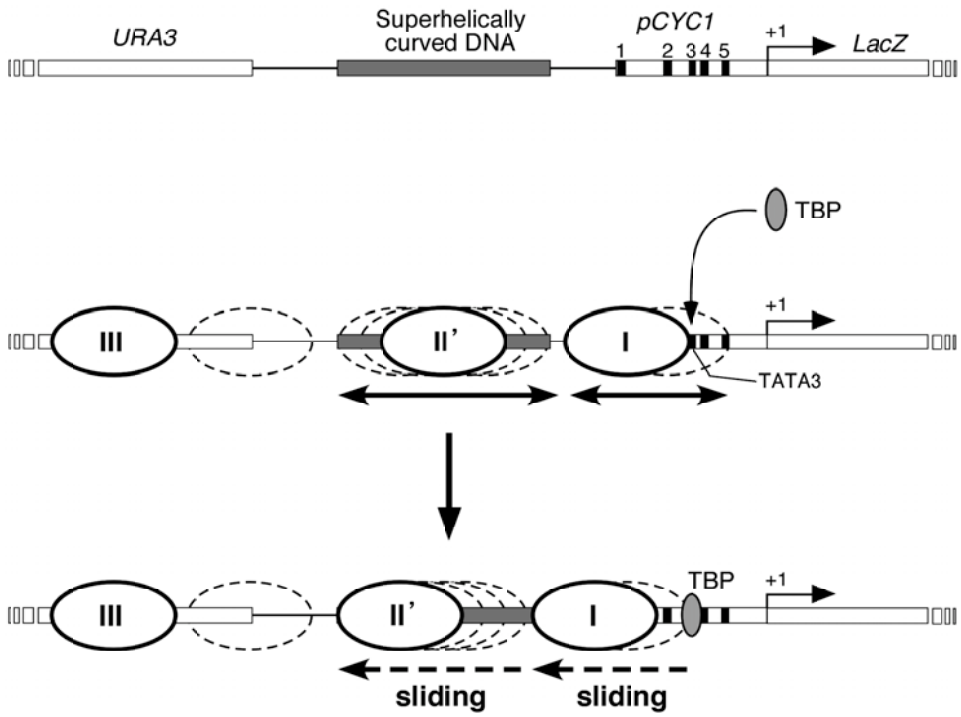

Fig. 26. The putative mechanism of transcriptional activation in chromatin induced by superhelically curved DNA structures

The high mobility of nucleosome II' on the curved DNA region generates a room to accept transiently and largely sliding nucleosome I that is caused by TBP binding, which exposes the promoter and activates transcription.

VIII. Acknowledgments

I greatly appreciate Prof. Takashi Ohyama (Department of Biology, School of Education, Waseda University, Tokyo, Japan) for his kind and appropriate advice and encouragement throughout this research.

I would like to express my gratitude to Prof. Toru Higashinakagawa, Prof. Hideo Namiki for the comment and discussion about this thesis. I would like to thank all collaborators, Dr. T. Mitani, Dr. M. Shimizu, Dr. J. Nishikawa, Dr. N. Morohashi Mr. K. Udagawa, Mr. H. Fujita, and Mr. S. Fujii. I would like to thank Dr. Y. Kadokawa for the plasmid pCX-GFP.

This work was supported in part by JSPS and MEXT research grants to T.O. and by a JSPS grant to M.S.

IX. References

1. Zahn, K., and Blattner, F. R. (1987) Direct evidence for DNA bending at the λ replication origin, *Science 236*, 416-422.
2. Hertz, G. Z., Young, M. R., and Mertz, J. E. (1987) The A+T-rich sequence of the simian virus 40 origin is essential for replication and is involved in bending of the viral DNA, *J. Virol. 61*, 2322-2325.
3. Williams, J. S., Eckdahl, T. T., and Anderson, J. N. (1988) Bent DNA functions as a replication enhancer in *Saccharomyces cerevisiae*, *Mol. Cell Biol. 8*, 2763-2769.
4. Inokuchi, K., Nakayama, and A., Hishinuma, F. (1988) Sequence-directed bends of DNA helix axis at the upstream activation sites of α-cell-specific genes in yeast, *Nucleic Acids Res. 16*, 6693-6711.
5. Ohyama, T., and Hashimoto, S. (1989) Upstream half of adenovirus type 2 enhancer adopts a curved DNA conformation, *Nucleic Acids Res. 17*, 3845-3853.
6. Travers, A. A. (1989) Curves with a function, *Nature* 341, 184-185.
7. Kawamoto, T., Makino, K., Orita, S., Nakata, A., and Kakunaga, T. (1989) DNA bending and binding factors of the human *ß-actin* promoter, *Nucleic Acids Res. 17*, 523-537.
8. Bedrosian, C. and L., Bastia, D. (1990) The DNA-binding domain of HPV-16 E2 protein interaction with the viral enhancer:

protein-induced DNA bending and role of the nonconserved core sequence in binding site affinity, *Virology 174*, 557-575.

9. Milot, E., Belmaaza, A., Wallenburg, J. C., Gusew, N., Bradley, W. E., and Chartrand, P. (1992) Chromosomal illegitimate recombination in mammalian cells is associated with intrinsically bent DNA elements, *EMBO J. 11*, 5063-5070.
10. Chang, Y. N., Jeang, K.T., Chiou, C. J., Chan, Y. J., Pizzorno, M., and Hayward, G. S. (1993) Identification of a large bent DNA domain and binding sites for serum response factor adjacent to the NFI repeat cluster and enhancer region in the major IE94 promoter from simian cytomegalovirus, *J. Virol. 67*, 516-529.
11. Perez-Martin, J., Rojo, F., and de Lorenzo, V. (1994) Promoters responsive to DNA bending: a common theme in prokaryotic gene expression, *Microbiol. Rev.* 58, 268-290.
12. Mazin, A., Milot, E., Devoret, R., and Chartrand, P. (1994) KIN17, a mouse nuclear protein, binds to bent DNA fragments that are found at illegitimate recombination junctions in mammalian cells, *Mol. Gen. Genet. 244*, 435-438.
13. Du, C., Sanzgiri, R. P., Shaiu, W. L., Choi, J. K., Hou, Z., Benbow, R. M., and Dobbs, D. L. (1995) Modular structural elements in the replication origin region of *Tetrahymena* rDNA, *Nucleic Acids Res. 23*, 1766-1774.

14. Polaczek, P., Kwan, K., Liberies, D. A., and Campbell, J. L. (1997) Role of architectural elements in combinatorial regulation of initiation of DNA replication in *Escherichia coli*, *Mol. Microbiol. 26*, 261-275.
15. Kusakabe, T., Sugimoto, Y., Hirota, Y., Toné, S., Kawaguchi, Y., Koga, K., and Ohyama, T. (2000) Isolation of replicational cue elements from a library of bent DNAs of *Aspergillus oryzae*. *Mol. Biol. Rep. 27*, 13-19.
16. Bash, R. C., Vargason, J. M., Cornejo, S., Ho, P. S., and Lohr, D. (2001) Intrinsically bent DNA in the promoter regions of the yeast *GAL1-10* and *GAL80* genes, *J. Biol. Chem. 276*, 861-866.
17. Miyano, M., Kawashima, T., and Ohyama, T. (2001) A common feature shared by bent DNA structures locating in the eukaryotic promoter region, *Mol. Biol. Rep. 28*, 53-61.
18. Ohyama, T. (2005) Curved DNA and Transcription in eukaryotes, in *DNA Conformation and Transcription* (Ohyama, T., Ed.), pp 66-74, Springer, New York.
19. Hagerman, P. J. (1990) Sequence-directed curvature of DNA, *Annu. Rev. Biochem. 59*, 755-781.
20. Ohyama, T. (2001) Intrinsic DNA bends: an organizer of local chromatin structure for transcription, *Bioessays 23*, 708-715.
21. Asayama, M., and Ohyama, T. (2005) Curved DNA and prokaryotic promoters: a mechanism for activation of transcription, in *DNA*

Conformation and Transcription (Ohyama, T., Ed), pp 37-51, Springer, New York.

22. Ohyama, T. (2005) The role of unusual DNA structures in chromatin organization for transcription, in *DNA Conformation and Transcription* (Ohyama, T., Ed), pp 177-188, Springer, New York.
23. Liu-Johnson, H. N., Gartenberg, M. R., and Crothers, D. M. (1986) The DNA binding domain and bending angle of *E. coli* CAP protein, *Cell 47*, 995-1005.
24. Plaskon, R. R., and Wartell, R. M. (1987) Sequence distributions associated with DNA curvature are found upstream of strong *E. coli* promoters, *Nucleic Acids Res. 15*, 785-796.
25. Bossi, L., and Smith, D. M. (1987) Conformational change in the DNA associated with an unusual promoter mutation in a tRNA operon of *Salmonella*, *Cell 39*, 643-652.
26. Bauer, B. F., Kar, E. G., Elford, R. M., and Holmes, W. M. (1988) Sequence determinants for promoter strength in the *leuV* operon of *Escherichia coli*, *Gene 63*, 123-134.
27. McAllister, C. F., and Achberger, E. C. (1989) Rotational orientation of upstream curved DNA affects promoter function in *Bacillus subtilis*, *J. Biol. Chem. 264*, 10451-10456.
28. Tanaka, K., Muramatsu, S., Yamada, H., and Mizuno, T. (1991) Systematic characterization of curved DNA segments randomly

cloned from *Escherichia coli* and their functional significance, *Mol. Gen. Genet. 226*, 367-376.

29. Zacharias, M., Theissen, G., Bradaczek, C., and Wagner, R. (1991) Analysis of sequence elements important for the synthesis and control of ribosomal RNA in *E. coli*, *Biochimie 73*, 699-712.
30. Hsu, L. M., Giannini, J. K., Leung, T. W., and Crosthwaite, J. C. (1991) Upstream sequence activation of *Escherichia coli argT* promoter *in vivo* and *in vitro*, Biochemistry 30, 813-822.
31. Ohyama, T., Nagumo, M., Hirota, Y., and Sakuma, S. (1992) Alteration of the curved helical structure located in the upstream region of the β-lactamase promoter of plasmid pUC19 and its effect on transcription, *Nucleic Acids Res. 20*, 1617-1622.
32. Wang, Q., Albert, F. G., Fitzgerald, D. J., Calvo, J. M., and Anderson, J. N. (1994) Sequence determinants of DNA bending in the *ilvlH* promoter and regulatory region of *Escherichia coli*, *Nucleic Acids Res. 22*, 5753-5760.
33. Hirota, Y., and Ohyama, T. (1995) Adjacent upstream superhelical writhe influences an *Escherichia coli* promoter as measured by *in vivo* strength and *in vitro* open complex formation, *J. Mol. Biol. 254*, 566-578.
34. Asayama, M., Yamamoto, A., and Kobayashi, Y. (1995) Dimer form of phosphorylated Spo0A, a transcriptional regulator, stimulates the

spo0F transcription at the initiation of sporulation in *Bacillus subtilis*, *J. Mol. Biol. 250*, 11-23.

35. Groß, S., Gase, K., and Malke, H. (1996) Localization of the sequence-determined DNA bending center upstream of the streptokinase gene *skc*, *Arch. Microbiol. 166*, 116-121.
36. Matsushita, C., Matsushita, O., Katayama, S., Minami, J., Takai, K., and Okabe, A. (1996) An upstream activating sequence containing curved DNA involved in activation of the *Clostridium perfringens plc* promoter, *Microbiology 142*, 2561-2566.
37. Asayama, M., Hayasaka, Y., Kabasawa, M., Shirai, M., and Ohyama, A. (1999) An intrinsic DNA curvature found in the cyanobacterium *Microcystis aeruginosa* K-81 affects the promoter activity of *rpoD1* encoding a principal σ factor, *J. Biochem. 125*, 460-468.
38. Mizuno, T. (1987) Static bend of DNA helix at the activator recognition site of the *ompF* promoter in *Escherichia coli*, *Gene 54*, 57-64.
39. Ross, W., Thompson, J. F., Newlands, J. T., and Gourse, R.L. (1990) *E. coli* Fis protein activates ribosomal RNA transcription *in vitro*, *EMBO J. 9*, 3733-3742.
40. Rojo, F., Zaballos, A., and Salas, M. (1990) Bend induced by the phage φ29 transcriptional activator in the viral late promoter is required for activation, *J. Mol. Biol. 211*, 713-725.

41. Kolb, A., Busby, S., Buc, H., Garges, S., and Adhya, S. (1993) Transcriptional regulation by cAMP and its receptor protein, *Annu. Rev. Biochem. 62*, 749-795.

42. Gaal, T., Rao, L., Estrem, S. T., Yang, J., Wartell, R. M., and Gourse, R. L. (1994) Localization of the intrinsically bent DNA region upstream of the *E. coli rrnB* P1 promoter, *Nucleic Acids Res. 22*, 2344-2350.

43. Carmona, M. and Magasanik, B. (1996) Activation of transcription at σ^{54}-dependent promoters on linear templates requires intrinsic or induced bending of the DNA, *J. Mol. Biol. 261*, 348-356.

44. Cheema, A. K., Choudhury, N. R., and Das, H. K. (1999) A- and T-tract-mediated intrinsic curvature in native DNA between the binding site of the upstream activator NtrC and the *nifLA* promoter of *Klebsiella pneumoniae* facilitates transcription, *J. Bacteriol. 181*, 5296-302.

45. Busby, S., Spassky, A., and Chan, B. (1987) RNA polymerase makes important contacts upstream from base pair -49 at the *Escherichia coli* galactose operon *P1* promoter, *Gene 53*, 145-152.

46. McAllister, C. F., and Achberger, E. C. (1988) Effect of polyadenine-containing curved DNA on promoter utilization in *Bacillus subtilis*, *J. Biol. Chem. 263*, 11743-11749.

47. Travers, A. A. (1990) Why bent DNA? *Cell 60*, 177-180.

48. Gartenberg, M. R., and Crothers, D. M. (1991) Synthetic DNA bending sequences increase the rate of *in vitro* transcription initiation at the *Escherichia coli lac* promoter, *J. Mol. Biol. 219*, 217-230.

49. Lavigne, M., Herbert, M., Kolb, A., and Buc, H. (1992) Upstream curved sequences influence the initiation of transcription at the *Escherichia coli* galactose operon, *J. Mol. Biol. 224*, 293-306.

50. Katayama, S., Matsushita, O., Jung, C. M., Minami, J., and Okabe, A. (1999) Promoter upstream bent DNA activates the transcription of the *Clostridium perfringens* phospholipase C gene in a low temperature-dependent manner, *EMBO J. 18*, 3442-3450.

51. Nickerson, C. A., and Achberger, E. C. (1995) Role of curved DNA in binding of *Escherichia coli* RNA polymerase to promoters, *J. Bacteriol. 177*, 5756-5761.

52. Nishikawa, J., Amano, M., Fukue, Y., Tanaka, S., Kishi, H., Hirota, Y., Yoda, K., and Ohyama, T. (2003) Left-handedly curved DNA regulates accessibility to *cis*-DNA elements in chromatin, *Nucleic Acids Res. 31*, 6651-6662.

53. Kamiya, H., Fukunaga, S., Ohyama, T., and Harashima, H. (2007) The location of the left-handedly curved DNA sequence affects exogenous DNA expression *in vivo*, *Arch. Biochem. Biophys. 461*, 7-12.

54. Kamiya, H., Fukunaga, S., Ohyama, T., and Harashima, H. (2009) Effects of carriers on transgene expression from plasmids containing a DNA sequence with high histone affinity, *Int. J. Pharm. 376*, 99-103.

55. Finch, J. T., Lutter, L. C., Rhodes, D., Brown, R. S., Rushton, B., Levitt, M., and Klug, A. (1977) Structure of nucleosome core particles of chromatin, *Nature 269*, 29-36.

56. Richmond, T. J., Finch, J. T., Rushton, B., Rhodes, D., and Klug, A. (1984) Structure of the nucleosome core particle at 7Å resolution, *Nature 311*, 532-537.

57. Angermayr, M., Oechsner, U., Gregor, K., Schroth, G. P., and Bandlow, W. (2002) Transcription initiation *in vivo* without classical transactivators: DNA kinks flanking the core promoter of the housekeeping yeast adenylate kinase gene, *AKY2*, position nucleosomes and constitutively activate transcription, *Nucleic Acids Res. 30*, 4199-4207.

58. Sumida, N., Sonobe, H., and Ohyama, T. (2007) Chromatin structure formed on a eukaryotic promoter activated by a left-handed superhelical bent DNA of 180 bp, *J. Adv. Sci. 19*, 22-28.

59. Li, B., Carey, M., and Workman, J. L. (2007) The role of chromatin during transcription, *Cell 128*, 707-719.

60. Morse, R. H. (2007) Transcription factor access to promoter elements, *J. Cell Biochem. 102*, 560-570.

61. Sumida, N., Nishikawa, J., Kishi, H., Amano, M., Furuya, T., Sonobe, H., and Ohyama, T. (2006) A designed curved DNA segment that is a remarkable activator of eukaryotic transcription, *FEBS J. 273*, 5691-5702.

62. Struhl, K., Stinchcomb, D. T., Scherer, S., and Davis, R. W. (1979) High-frequency transformation of yeast: autonomous replication of hybrid DNA molecules, *Proc. Natl. Acad. Sci. U.S.A. 76*, 1035-1039.

63. Reid, L. H., Shesely, E. G., Kim, H. S., and Smithies, O. (1991) Cotransformation and gene targeting in mouse embryonic stem cells, *Mol. Cell Biol. 11*, 2769-2777.

64. Piedrahita, J. A., Zhang, S. H., Hagaman, J. R., Oliver, P. M., and Maeda, N. (1992) Generation of mice carrying a mutant apolipoprotein E gene inactivated by gene targeting in embryonic stem cells, *Proc. Natl. Acad. Sci. U.S.A. 89*, 4471-4475.

65. Rubinstein, M., Japon, M. A., and Low, M. J. (1993) Introduction of a point mutation into the mouse genome by homologous recombination in embryonic stem cells using a replacement type vector with a selectable marker, *Nucleic Acids Res. 21*, 2613-2617.

66. Detloff, P. J., Lewis, J., John, S. W., Shehee, W. R., Langenbach, R., Maeda, N., and Smithies, O. (1994) Deletion and replacement of the mouse adult *ß-globin* genes by a "plug and socket" repeated targeting strategy, *Mol. Cell Biol. 14*, 6936-6943.

67. Araki, K., Araki, M., and Yamamura, K. (1997) Targeted integration of DNA using mutant *lox* sites in embryonic stem cells, *Nucleic Acids Res. 25*, 868-872.

68. Yamada, T., Yoshikawa, M., Kanda, S., Kato, Y., Nakajima, Y., Ishizaka, S., and Tsunoda, Y. (2002) *In vitro* differentiation of

embryonic stem cells into hepatocyte-like cells identified by cellular uptake of indocyanine green, *Stem Cells 20*, 146-154.

69. Teng, L., Meng, G., Xing, Y., Shang, K., Wang, X., and Gu, J. (2003) Labeling embryonic stem cells with enhanced green fluorescent protein on the hypoxanthineguanine phosphoribosyl transferase locus, *Chin. Med. J. 116*, 267-272.
70. Ochman, H., Gerber, A. S., and Hart, D. L. (1988) Genetic aplications of an inverse polymerase chain reaction, *Genetics 120*, 621-623.
71. Teratani, T., Yamamoto, H., Aoyagi, K., Sasaki, H., Asari, A., Quinn, G., Sasaki, H., Terada, M., and Ochiya, T. (2005) Direct hepatic fate specification from mouse embryonic stem cells, *Hepatology 41*, 836-846.
72. Lavon, N., and Benvenisty, N. (2005) Study of hepatocyte differentiation using embryonic stem cells, *J. Cell Biochem. 96*, 1193-1202.
73. Pfeifer, G. P., Chen, H. H., Komura, J., and Riggs, A. D. (1999) Chromatin structure analysis by ligation-mediated and terminal transferase-mediated polymerase chain reaction, *Methods Enzymol. 304*, 548-571.
74. Chadee, D. N., Hendzel, M. J., Tylipski, C. P., Allis, C. D., Bazett-Jones, D. P., Wright, J. A., and Davie, J. R. (1999) Increased Ser-10 phosphorylation of histone H3 in mitogen-stimulated and

oncogene-transformed mouse fibroblasts, *J. Biol. Chem. 274*, 24914-24920.

75. Sternberg, N., and Hamilton, D. (1981) Bacteriophage P1 site-specific recombination I. Recombination between *loxP* sites, *J. Mol. Biol. 150*, 467-486.
76. Sternberg, N., Hamilton, D., and Hoess, R. (1981) Bacteriophage P1 site-specific recombination II. Recombination between *loxP* and the bacterial chromosome, *J. Mol. Biol. 150*, 487-507.
77. Hoess, R. H., Ziese, M., and Sternberg, N. (1982) P1 site-specific recombination: nucleotide sequence of the recombining sites, *Proc. Natl. Acad. Sci. U.S.A. 79*, 3398-3402.
78. Sauer, B., and Henderson, N. (1989) Cre-stimulated recombination at *loxP*-containing DNA sequences placed into the mammalian genome, *Nucleic Acids Res. 17*, 147-161.
79. Rickert, R. C., Roes, J., and Rajewsky, K. (1997) B lymphocyte-specific, Cre-mediated mutagenesis in mice, *Nucleic Acids Res. 25*, 1317-1318.
80. Mullins, L. J., Kotelevtseva, N., Boyd, A. C., and Mullins, J. J. (1997) Efficient Cre-*lox* linearisation of BACs: applications to physical mapping and generation of transgenic animals, *Nucleic Acids Res. 25*, 2539-2540.

81. Sauer, B., and Henderson, N. (1998) Site-specific DNA recombination in mammalian cells by the Cre recombinase of bacteriophage P1, *Proc. Natl. Acad. Sci. U.S.A. 85*, 5166-5170.

82. Kost, T. A., Theodorakis, N., and Hughes, S. H. (1983) The nucleotide sequence of the chick cytoplasmic *ß-actin* gene, *Nucleic Acids Res. 11*, 8287-8301.

83. Miyazaki, J., Takaki, S., Araki, K., Tashiro, F., Tominaga, A., Takatsu, K., and Yamamura, K. (1989) Expression vector system based on the chicken *ß-actin* promoter directs efficient production of interleukin-5, *Gene 79*, 269-277.

84. Sawicki, J. A., Morris, R. J., Monks, B., Sakai, K., and Miyazaki, J. (1998) A composite CMV-IE enhancer/*ß-actin* promoter is ubiquitously expressed in mouse cutaneous epithelium, *Exp. Cell Res. 244*, 367-369.

85. Chung, S., Andersson, T., Sonntag, K. C., Björklund, L., Isacson, O., and Kim, K. S. (2002) Analysis of different promoter systems for efficient transgene expression in mouse embryonic stem cell lines, *Stem Cells 20*, 139-145.

86. Zhu, D. Y., Du, Y., Huang, X., Guo, M. Y., Ma, K. F., Yu, Y. P., and Lou, Y. J. (2008) MAPEG expression in mouse embryonic stem cell-derived hepatic tissue system, *Stem Cells Dev. 17*, 775-783.

87. Malcuit, C., Trask, M. C., Santiago, L., Beaudoin, E., Tremblay, K. D., and Mager, J. (2009) Identification of novel oocyte and granulosa cell markers, *Gene Expr. Patterns 9*, 404-410.

88. Sharova, L. V., Sharov, A. A., Nedorezov, T., Piao, Y., Shaik, N., and Ko, M. S. (2009) Database for mRNA Half-Life of 19 977 genes obtained by DNA microarray analysis of pluripotent and differentiating mouse embryonic stem cells, *DNA Res. 16*, 45-48.

89. Stenvers, K. L., Tursky, M. L., Harder, K. W., Kountouri, N., Amatayakul-Chantler, S., Grail, D., Small, C., Weinberg, R. A., Sizeland, A. M., and Zhu, H. J. (2003) Heart and liver defects and reduced transforming growth factor β2 sensitivity in transforming growth factor β type III receptor-deficient embryos, *Mol. Cell Biol. 23*, 4371-4385.

90. Lilley, D. M., Gough, G. W., Hallam, L. R., and Sullivan, K. M. (1985) The physical chemistry of cruciform structures in supercoiled DNA molecules. *Biochimie 67*, 697-706.

91. Nobile, C., Nickol, J., and Martin, R. G. (1986) Nucleosome phasing on a DNA fragment from the replication origin of simian virus 40 and rephasing upon cruciform formation of the DNA, *Mol. Cell Biol. 6*, 2916-2922.

92. Kotani, H., and Kmiec, E. B. (1994) DNA cruciforms facilitate *in vitro* strand transfer on nucleosomal templates, *Mol. Gen. Genet. 243*, 681-690.

93. Bowdish, K. S., and Mitchell, A. P. (1993) Bipartite structure of an early meiotic upstream activation sequence from *Saccharomyces cerevisiae*, *Mol. Cell Biol. 13*, 2172-2181.

94. Guarente, L., and Mason, T. (1983) Heme regulates transcription of the *CYC1* gene of *S. cerevisiae* via an upstream activation site, *Cell 32*, 1279-l286.

95. Burke, D., Dawson, D., and Stearns, T. (2000) *Methods in Yeast Genetics: A Laboratory Course Manual*, Cold Spring Harbor Lab. Press, Plainview, N.Y.

96. Shimizu, M., Roth, S. Y., Szent-Gyorgyi, C., and Simpson, R. T. (1991) Nucleosomes are positioned with base pair precision adjacent to the α operator in *Saccharomyces cerevisiae*, *EMBO J. 10*, 3033-3041.

97. Shimizu, M., Mori, T., Sakurai, T., and Shindo, H. (2000) Destabilization of nucleosomes by an unusual DNA conformation adopted by poly(dA)・(dT) tracts *in vivo*, *EMBO J. 19*, 3358-3365.

98. Kuo, M. H., and Allis, C. D. (1999) *In vivo* cross-linking and immunoprecipitation for studying dynamic Protein:DNA associations in a chromatin environment, *Methods 19*, 425-433.

99. Han, M., and Grunstein, M. (1988) Nucleosome loss activates yeast downstream promoters *in vivo*, *Cell 55*, 1137-1145.

100. Nedospasov, S. A., and Georgiev, G. P. (1980) Non-random cleavage of SV40 DNA in the compact minichromosome and free in solution

by micrococcal nuclease, *Biochem. Biophys. Res. Commun. 92*, 532-539.

101. Wu, C. (1980) The 5' ends of *Drosophila* heat shock genes in chromatin are hypersensitive to DNase I, *Nature 286*, 854-860.
102. Horz, W., and Altenburger, W. (1981) Sequence specific cleavage of DNA by micrococcal nuclease, *Nucleic Acids Res. 9*, 2643-2658.
103. Dingwall, C., Lomonossoff, G. P., and Laskey, R. A. (1981) High sequence specificity of micrococcal nuclease, *Nucleic Acids Res. 9*, 2659-2673.
104. Thoma, F., Bergman, L. W., and Simpson, R. T. (1984) Nuclease digestion of circular TRP1ARS1 chromatin reveals positioned nucleosomes separated by nuclease-sensitive regions, *J. Mol. Biol. 177*, 715-733.
105. Tanaka, S., Livingstone-Zatchej, M., and Thoma, F. (1996) Chromatin structure of the yeast *URA3* gene at high resolution provides insight into structure and positioning of nucleosomes in the chromosomal context, *J. Mol. Biol. 257*, 919-934.
106. Li W. Z., and Sherman, F. (1991) Two types of TATA elements for the *CYC1* gene of the yeast *Saccharomyces cerevisiae*, *Mol. Cell Biol. 11*, 666-676.
107. Hahn, S., Hoar, E.T., and Guarente, L. (1985) Each of three "TATA elements" specifies a subset of the transcription initiation sites at the

CYC-1 promoter of *Saccharomyces cerevisiae*, *Proc. Natl. Acad. Sci. U.S.A. 82*, 8562-8566.

108. Pennings, S., Muyldermans, S., Meersseman, G., and Wyns, L. (1989) Formation, stability and core histone positioning of nucleosomes reassembled on bent and other nucleosome-derived DNA, *J. Mol. Biol. 207*, 183-192.

109. Pina, B., Barettino, D., Truss, M., and Beato, M. (1990) Structural features of a regulatory nucleosome, *J. Mol. Biol. 216*, 975-990.

110. Costanzo, G., Di Mauro, E., Salina, G., and Negri, R. (1990) Attraction, phasing and neighbour effects of histone octamers on curved DNA, *J. Mol. Biol. 216*, 363-374.

111. Shrader, T. E., and Crothers, D. M. (1990) Effects of DNA sequence and histone-histone interactions on nucleosome placement, *J. Mol. Biol. 216*, 69-84.

112. Widlund, H. R., Cao, H., Simonsson, S., Magnusson, E., Simonsson, T., Nielsen, P. E., Kahn, J. D., Crothers, D. M., and Kubista, M. (1997) Identification and characterization of genomic nucleosome-positioning sequences, *J. Mol. Biol. 267*, 807-817.

113. Meersseman, G., Pennings, S., and Bradbury, E. M. (1992) Mobile nucleosomes--a general behavior, *EMBO J. 11*, 2951-2959.

114. Jiang C. and Pugh B. F. (2009) Nucleosome positioning and gene regulation: advances through genomics, *Nat. Rev. Genet.10*, 161-172.

115. Lomvardas, S., and Thanos, D. (2001) Nucleosome sliding via TBP DNA binding *in vivo*, *Cell 106*, 685-696.

研究業績

（２０１０年　３月　現在）

種 類 別	題名、　発表・発行掲載誌名、　発表・発行年月、　連名者（申請者含む）
論文　○	1. Tanase J., Morohashi N., Fujita M., Nishikawa J., Shimizu M., Ohyama T. Highly efficient chromatin transcription induced by superhelically curved DNA segments: the underlying mechanism revealed by a yeast system (2010) *Biochemistry* 49, 2351-2358.
○	2. Tanase J., Mitani T., Udagawa K., Nishikawa J., Ohyama T. Competence of an artificial bent DNA as a transcriptional activator in mouse ES cells (2010) *Mol. Biol. Rep.* in press.
	3. Fukue Y., Sumida N., Tanase J., Ohyama T. A highly distinctive mechanical property found in the majority of human promoters and its transcriptional relevance. (2005) *Nucl. Acids. Res.* 33, 3821-3827.
講演　○	1. Tanase J., Udagawa K., Ohyama T. Stable transgene expression based on chromatin engineering. The Wilhelm Bernhard Workshop 21st International Workshop on the cell Nucleus 2009 Sep. Ustron, Poland
	2. Ohyama T., Kimura H., Shimooka Y., Kageyama D., Furuya M., Udagawa K., Tanase J. How genomic DNA is functionally folded in a nucleus. The Wilhelm Bernhard Workshop 21st International Workshop on the cell Nucleus 2009 Sep. Ustron, Poland
	3. Ohyama T., Tanase J., Kimura H. Genetic information carried in DNA conformation and properties. EMBO Conference Series on Nuclear Structure and Dynamics 2007 Aug. Montpelier
	4. Ohyama T., Sumida N., Tanase J. How promoters are recognized. 7th EMBL Transcription Meeting. 2006 Aug. Heidelberg
	5. Fukue Y., Sumida N., Tanase J., Ohyama T. Mechanical properties of DNA: how eukaryotic promoters are recognized. International Symposium on Ran and Cell Cycle 2005 Oct. Awaji
○	6. 棚瀬潤一、宇田川紘司、西川純一、三谷匡、大山隆．クロマチン工学による外来遺伝子の安定的発現．第 32 回日本分子生物学会年会 2009 年 12 月　横浜
	7. 伊藤美月、棚瀬潤一、山内恵里、清水光弘、大山隆．遺伝子発現に有利なクロマチン構造の人為的構築. 第 32 回日本分子生物学会年会 2009 年 12 月　横浜
	8. 藤田仁、諸橋伸行、棚瀬潤一、大山隆、清水光弘．出芽酵母における DNA 構造による遺伝子発現とクロマチン構造の制御. 第 32 回日本分子生物学会年会 2009 年 12 月　横浜

	9. 宇田川紘司、山本拓弥、棚瀬潤一、深川竜郎、大山隆. 人工ベント DNA により活性化されたトランスジーンの核内局在：マウス ES 細胞を用いた解析. 第 32 回日本分子生物学会年会 2009 年 12 月　横浜 10. 宇田川紘司、山本拓弥、棚瀬潤一、深川竜郎、大山隆. マウス ES 細胞における高発現トランスジーンの核内配置. 第 26 回染色体ワークショップ 2009 年 1 月　姫路 11. 伊藤美月、棚瀬潤一、山内恵里、清水光弘、大山隆. 遺伝子発現に有利なクロマチン構造の人為的構築. 第 31 回日本分子生物学会年会 第 81 回日本生化学会年会合同大会 2008 年 12 月　神戸 12. 藤田仁、諸橋伸行、棚瀬潤一、大山隆、清水光弘. DNA 構造によるクロマチンの改変と人為的遺伝子発現制御：出芽酵母レポータープラスミドによる解析. 第 31 回日本分子生物学会年会 第 81 回日本生化学会年会合同大会 2008 年 12 月　神戸
○	13. 棚瀬潤一、宇田川紘司、山本拓弥、伊藤美月、藤井俊輔、三谷匡、大山隆. クロマチン工学による外来遺伝子の安定的発現. 第30回日本分子生物学会年会 第80回日本生化学会年会合同大会 2007年12月　横浜 14. 大山隆、棚瀬潤一、伊藤美月、三谷匡、清水光弘. クロマチン工学のストラテジー. 第 30 回日本分子生物学会年会 第 80 回日本生化学会年会合同大会 2007 年 12 月　横浜 15. 三谷匡、川村紘子、笹栗弘貴、横田隆徳、棚瀬潤一、大山隆、田口善智. マウス ES 細胞における非 B-型 DNA による shRNA 発現活性化に対する効果. 第 30 回日本分子生物学会年会 第 80 回日本生化学会年会合同大会 2007 年 12 月　横浜. 16. 大山隆、棚瀬潤一、宇田川紘司、木村元、景山大、古屋美香、藤井俊輔、三谷匡. ゲノム DNA の特性解析と高次遺伝情報の解読. 第 7 回核ダイナミクス研究会 2007 年 9 月　北海道 17. Ohyama T., Sumida N., Fukue Y., Tanase J., Inoue S.　Genetic information written in DNA conformation and properties. 第29回日本分子生物学会年会 第 79 回日本生化学会年会合同大会 2006 年 6 月 京都 18. 大山隆、 隅田周志、 棚瀬潤一. クロマチン工学の開拓. 第 6 回細胞核ダイナミクス研究会 2006 年 5 月　熊本
○	19. 棚瀬潤一、 隅田周志、大山隆. クロマチン基盤構造の局所的改変とその遺伝子発現への影響. 第 28 回日本分子生物学会年会 2005 年 12 月　福岡 20. Fukue Y., Sumida N., Tanase J., Motoyama T., Inoue S., Ohyama T. A highly

	distinctive mechanical property common to human promoters and its transcriptional relevance. 第 28 回日本分子生物学会年会 2005 年 12 月 福岡 21. 大山隆、 福江善朗、 井上正太郎、 隅田周志、 棚瀬潤一. DNA に印された配列以外の情報を読む. 生理研研究会 2005 年 11 月　岡崎 22. 隅田周志、 棚瀬潤一、 古屋貴代、 大山隆. クロマチン内 DNA の回転的ポジショニングと遺伝子発現. 第 27 回日本分子生物学会年会 2004 年 12 月　神戸
著書	1. Ohyama T., Sumida N., Tanase J., Ino 1 1 ue S., Okabe T. (2006) Genetic information carried in DNA conformation and properties. *DNA STRUCTUERE, CHROMATIN AND EXPRESSION* pp.71-84 Transworld Research Network (Kerala)